# Nonequilibrium dynamical mean field theory

Philipp Werner

University of Fribourg

College de France, May 2019

# Motivation

## Ultrafast pump-probe spectroscopy

- Time resolution: ~10 fs $\longrightarrow$ measures excitation and relaxation processes on the intrinsic timescale of the electrons

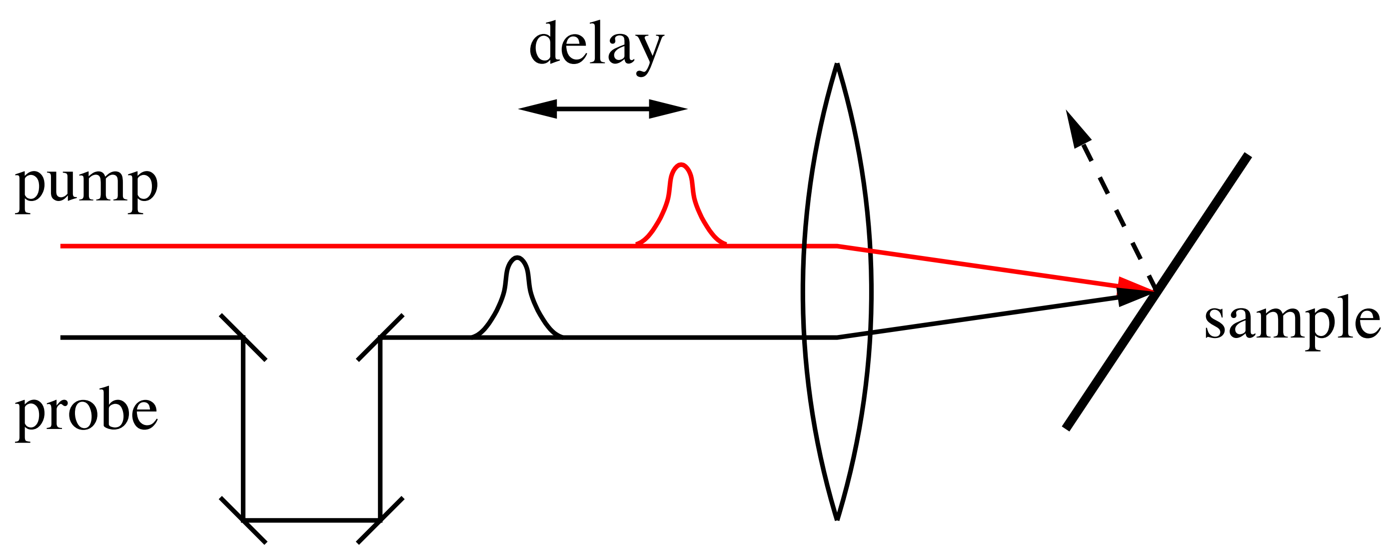


  - Pump pulse drives system out of equilibrium
  - Time evolution measured by subsequent probe pulses

- “Disentangles” competing or cooperative effects on the time-axis

# Motivation

## “Tuning” of material properties by external driving

- Ultra-fast insulator-metal transition (“photo-doping”)

  *Iwai et al. (2003)*

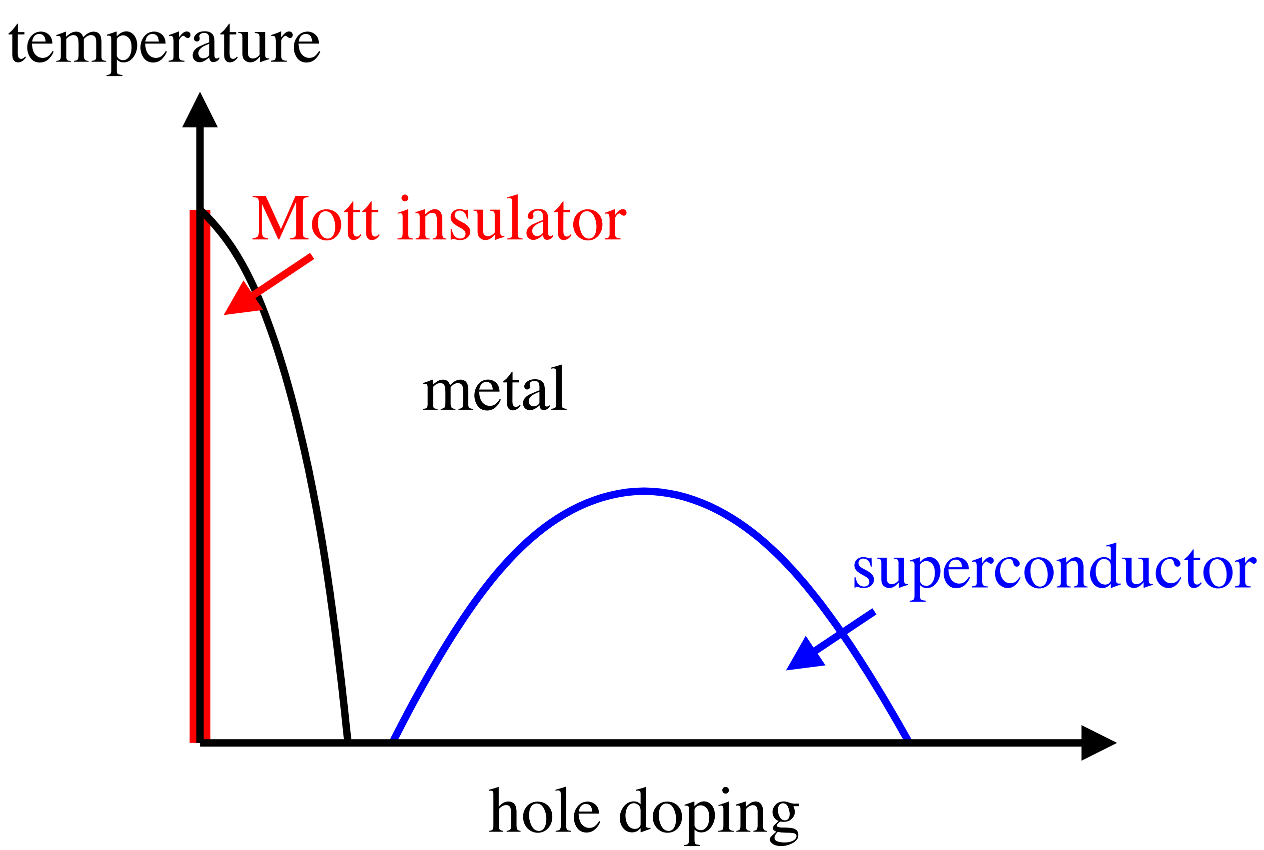


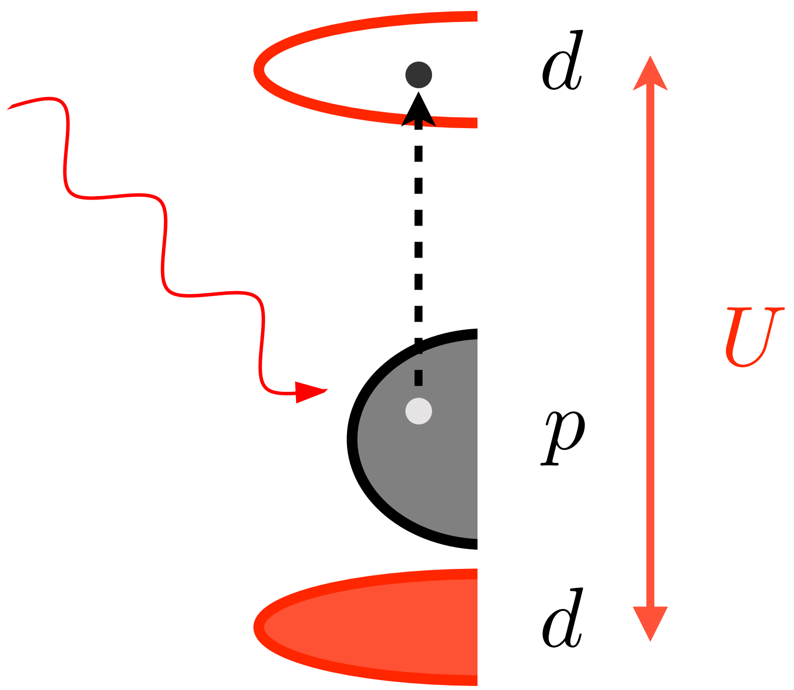

# Motivation

“Tuning” of material properties by external driving

- Create long-lived transient states with novel properties

  e. g. *light-induced high-temperature superconductivity*

  *Fausti et al. (2010), Kaiser et al. (2013)*

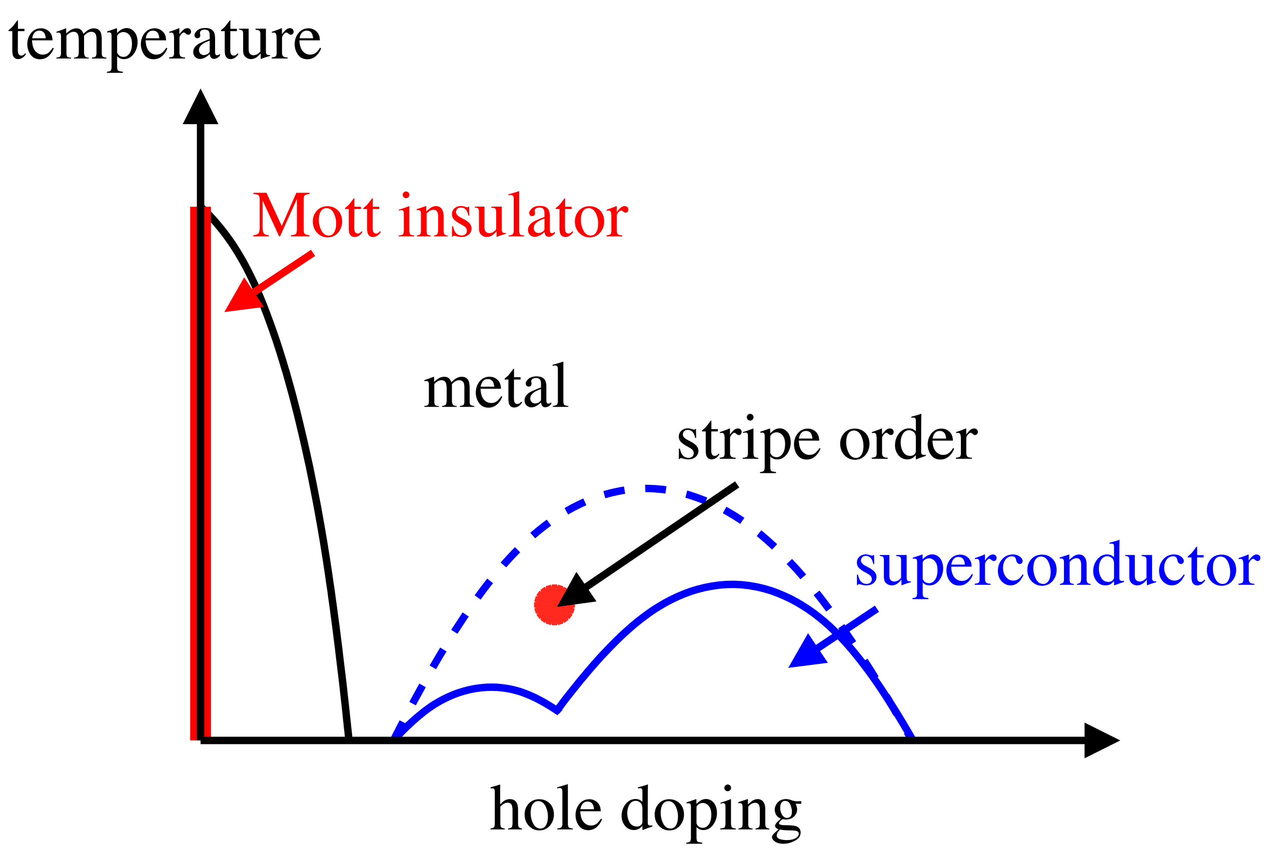


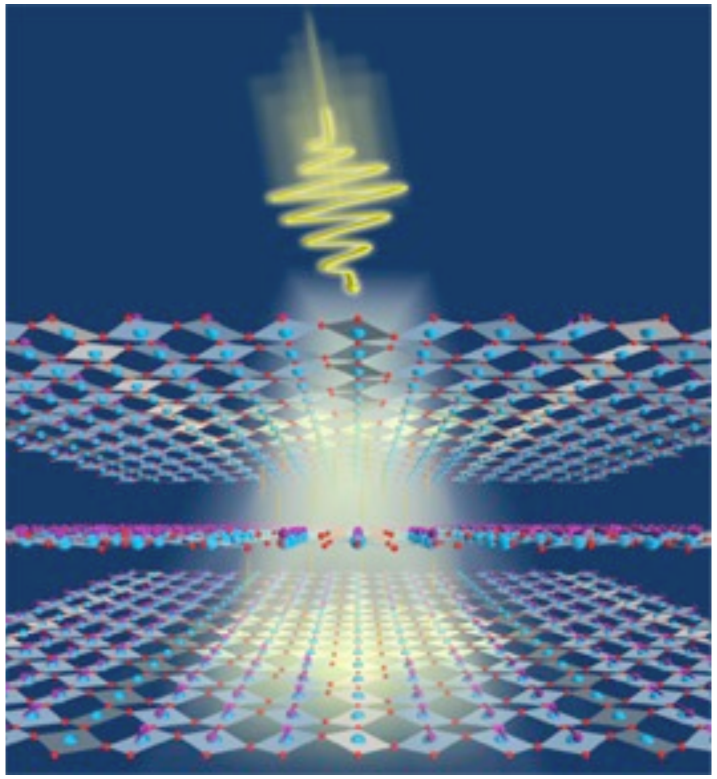

*THz pulse couples to phonons*

# Motivation

"Tuning" of material properties by external driving

- Create long-lived transient states with novel properties

  e. g. *light-induced high-temperature superconductivity*

*Mitrano et al. (2015)*

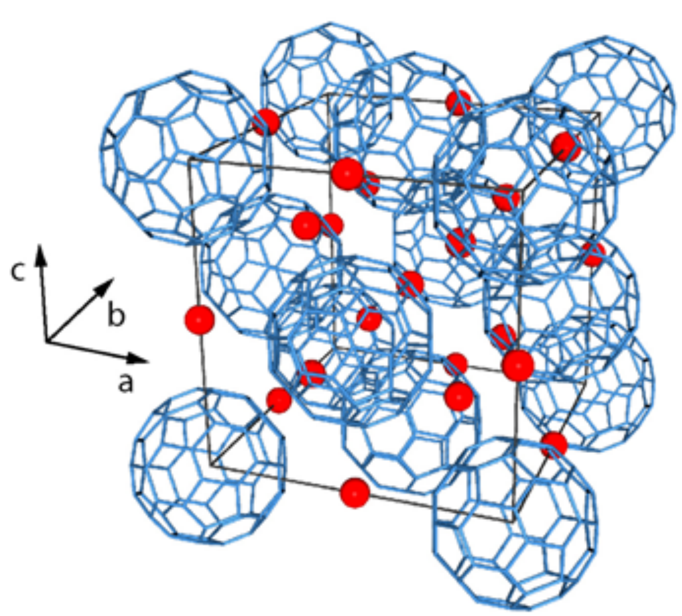


*$K_3C_{60}$*

*equilibrium*

*driven phonons*

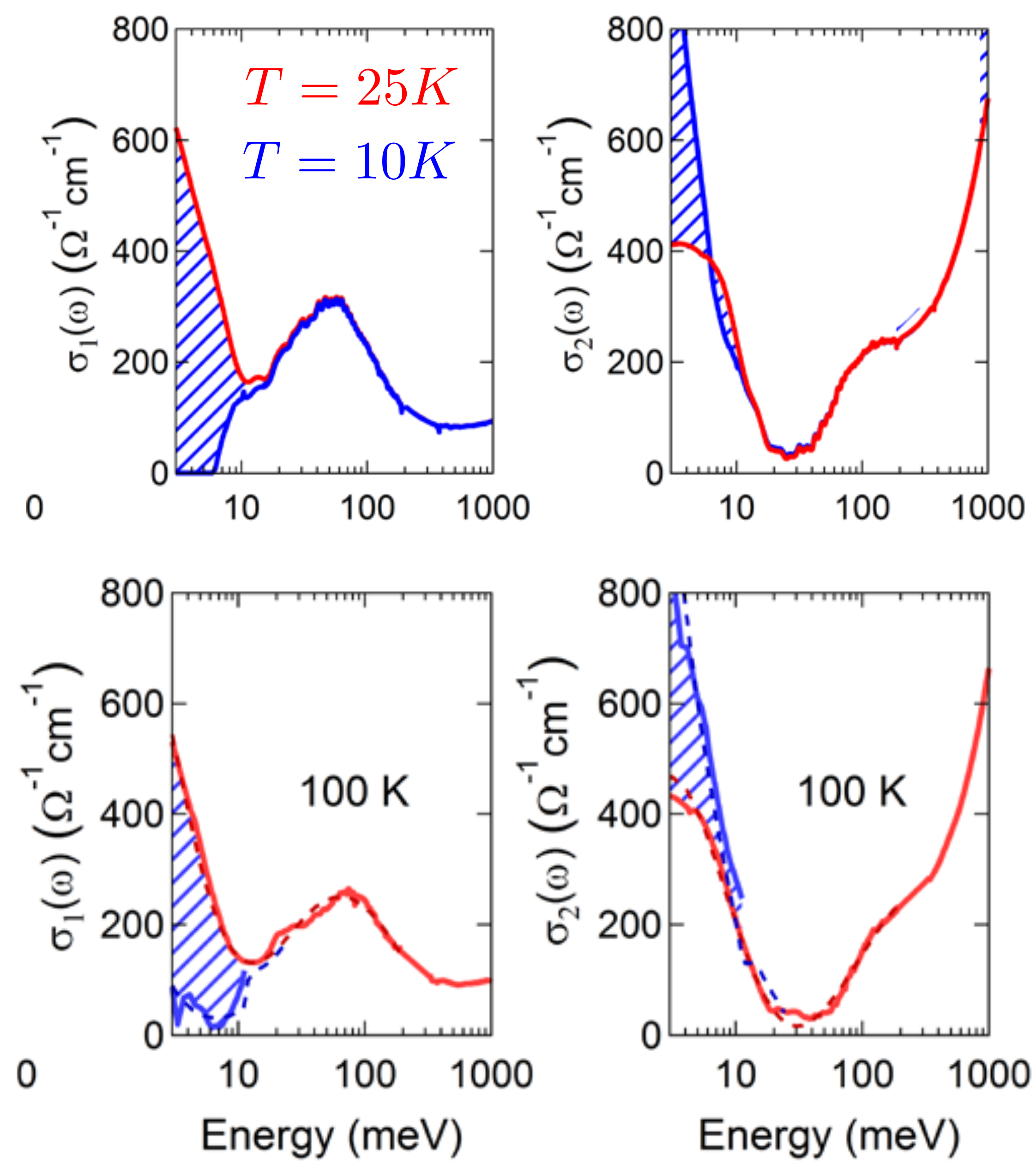

# Motivation

“Tuning” of material properties by external driving

- Switching into metastable, but long-lived “hidden states”

  e. g. *Reversible switching of $TaS_2$ into / out of a metallic hidden state*

  *Stojchevska et al. (2015)*

*equilibrium state (insulating)*

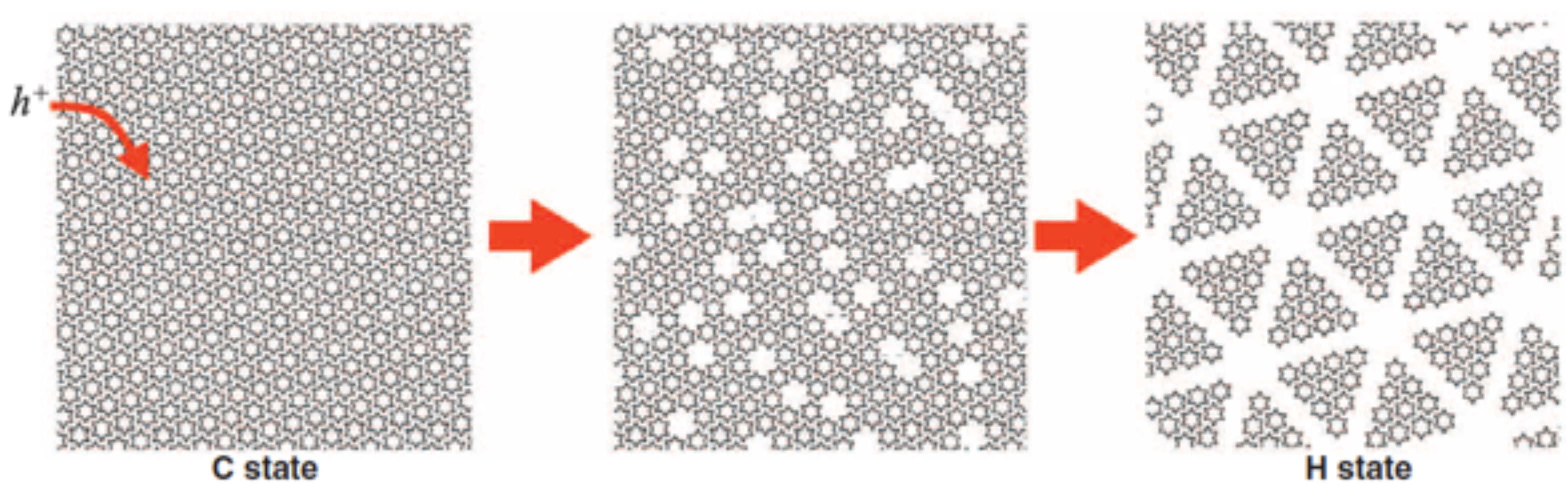


*hidden state (conducting)*

# Motivation

- Challenge for theory/numerics

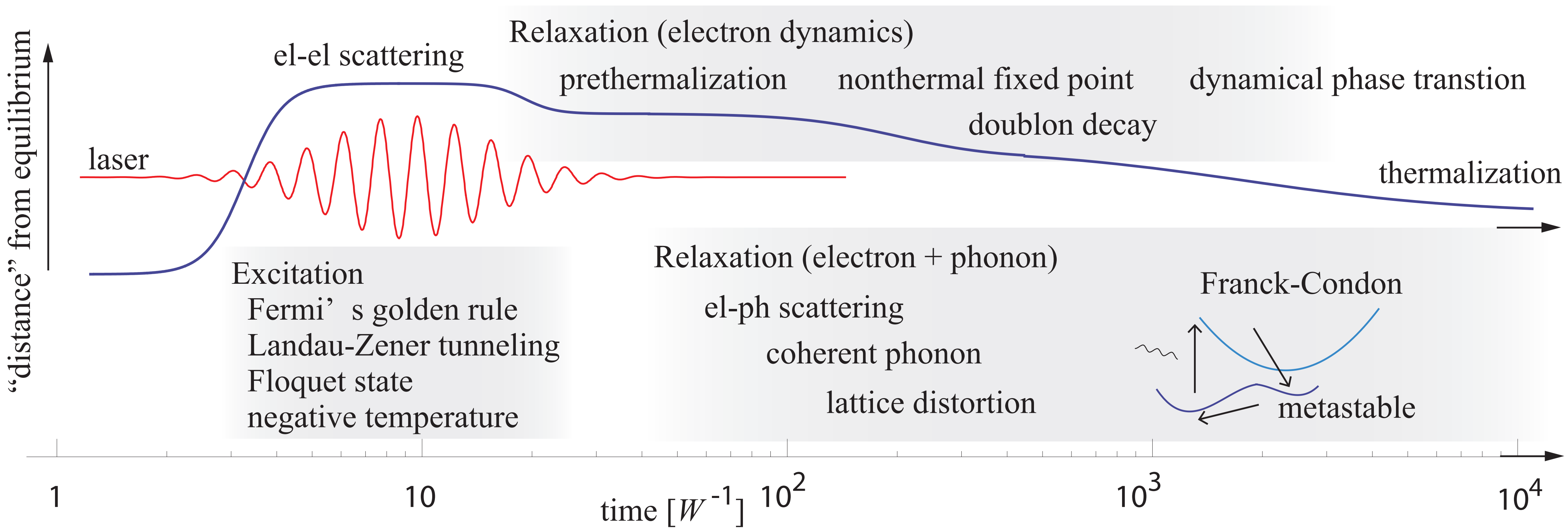


- Strongly interacting many-particle system
- Strong perturbations
- Different relevant time scales

# Overview

- *Dynamical mean field theory*
- *Nonequilibrium extension*
- *Physical observables*
- *Illustrations:*
    - *AC field quench - tuning of the interaction strength by external driving*
    - *Nonequilibrium phase transition - nonthermal fixed points*

# Model and method

- Static mean field theory: mapping to a single-site problem

  *Weiss (1903)*

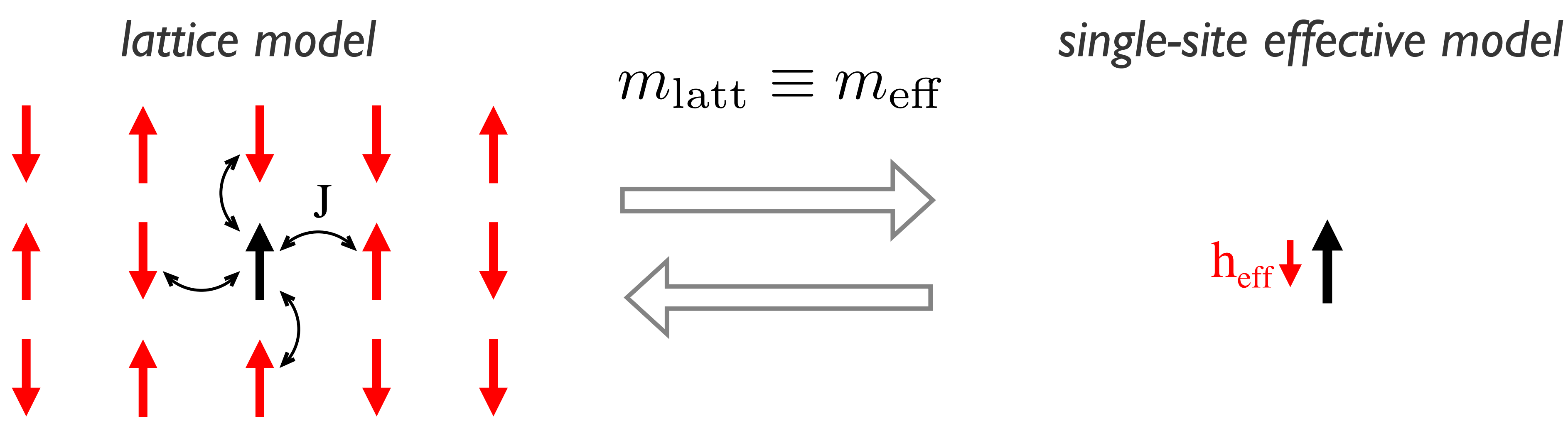


- Effective model: yields local observables (magnetization)

- Parameter of the effective model ("mean field"): optimized by requesting consistency between the lattice and single-site model

# Model and method

- Dynamical mean field theory DMFT: mapping to an impurity problem

  *Georges & Kotliar (1992)*

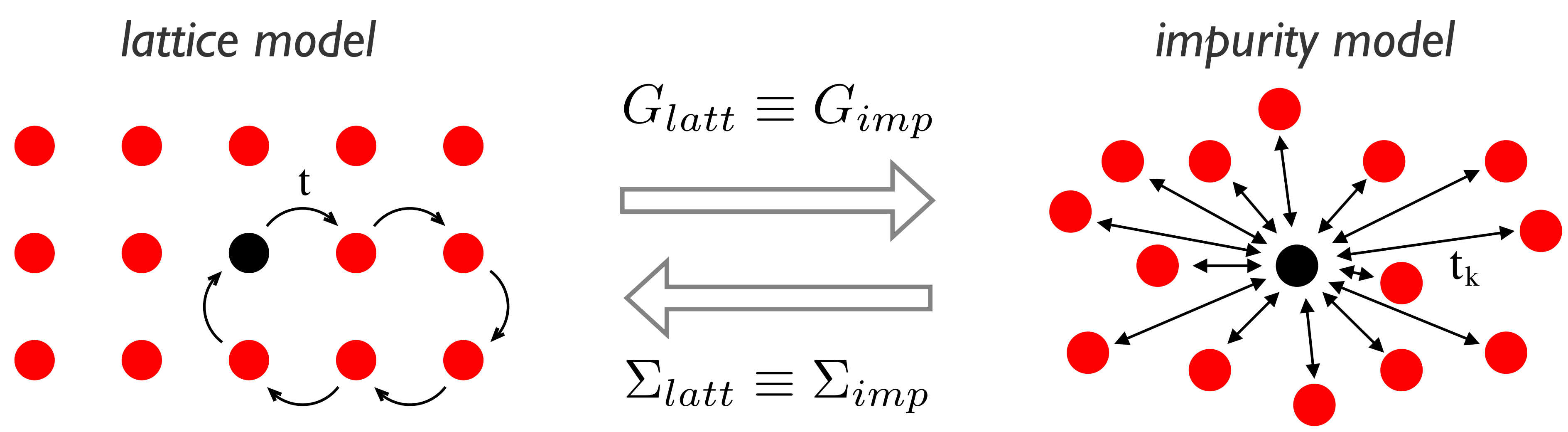


- Impurity solver: computes the Green's function of the correlated site

- Bath parameters = "mean field": optimized in such a way that the bath mimics the lattice environment

# Model and method

- Dynamical mean field theory DMFT: mapping to an impurity problem

  *Georges & Kotliar (1992)*

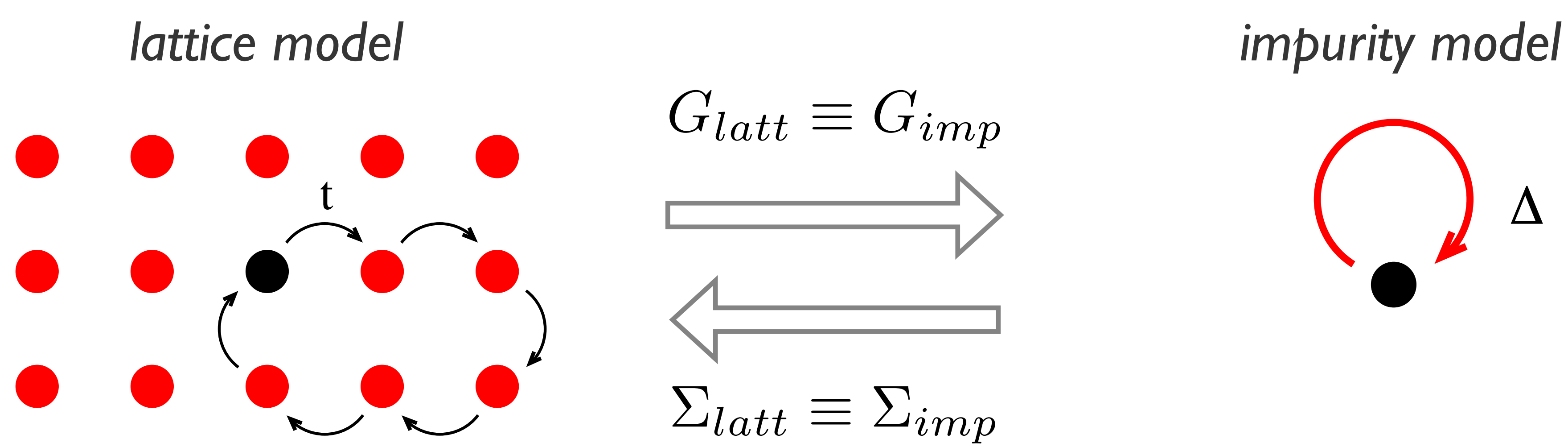


- Impurity solver: computes the Green's function of the correlated site

- Bath parameters = "mean field": optimized in such a way that the bath mimics the lattice environment

# Model and method

- Dynamical mean field theory DMFT: mapping to an impurity problem

  *Georges & Kotliar (1992)*

*lattice model* *impurity model*

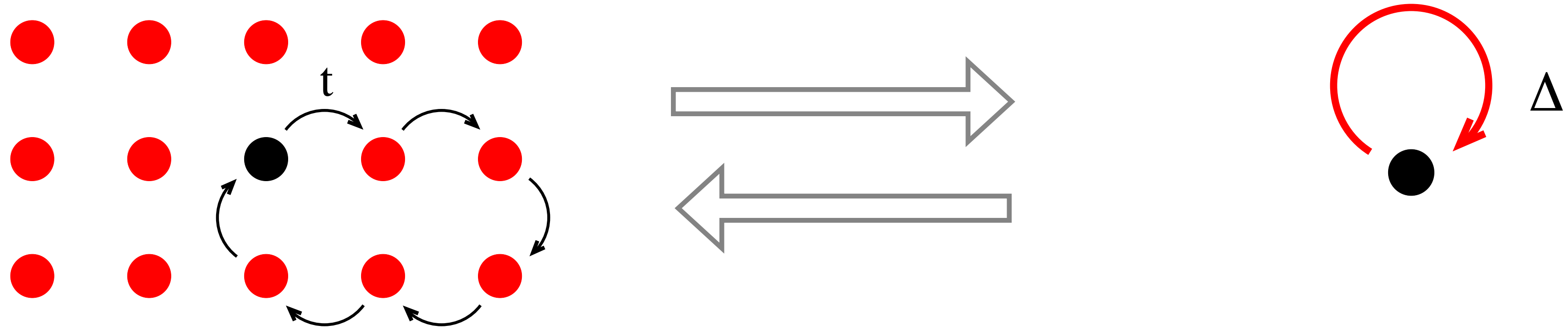


*DMFT self-consistency*

$$G^{\rm latt}_{\rm loc}(i\omega_n) \quad \Longrightarrow \quad S_{\rm imp}[\Delta(i\omega_n)]$$

$$G^{\rm latt}_{\rm loc} \equiv G_{\rm imp}$$

*momentum average* *impurity solver*

$$\Sigma^{\rm latt}_k \equiv \Sigma_{\rm imp}$$

$$G^{\rm latt}_k = \frac{1}{i\omega_n + \mu - \epsilon_k - \Sigma^{\rm latt}_k} \quad \Longleftarrow \quad G_{\rm imp}(i\omega_n), \Sigma_{\rm imp}(i\omega_n)$$

*DMFT approximation*

# Model and method

- Dynamical mean field theory DMFT: mapping to an impurity problem

  *Georges & Kotliar (1992)*

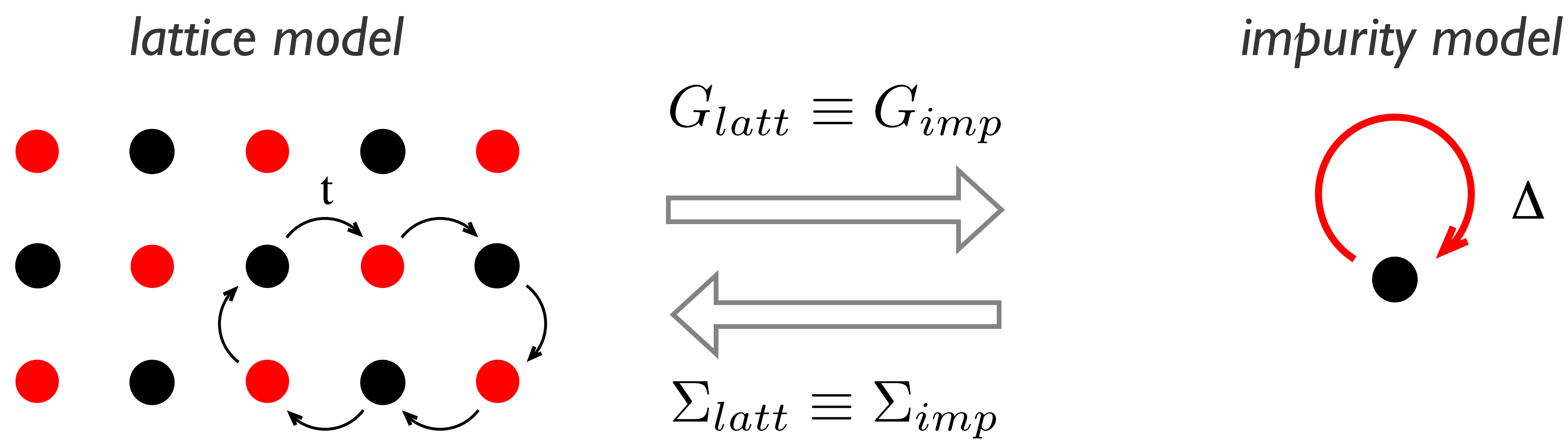


- Single-site DMFT can treat two-sublattice order (e. g. AFM)

$$\mathrm{Bath}_{B,\sigma}[G_{A,\sigma}], \quad \mathrm{Bath}_{A,\sigma}[G_{B,\sigma}]$$

- Pure Neel order: $\mathrm{Bath}_{B,\sigma} = \mathrm{Bath}_{A,\bar{\sigma}} \;\longrightarrow\; \mathrm{Bath}_{A,\bar{\sigma}}[G_{A,\sigma}]$

# Model and method

- Equilibrium DMFT phase diagram (half-filling)
- Paramagnetic calculation: Metal - Mott insulator transition at low *T*
- Smooth crossover at high *T*

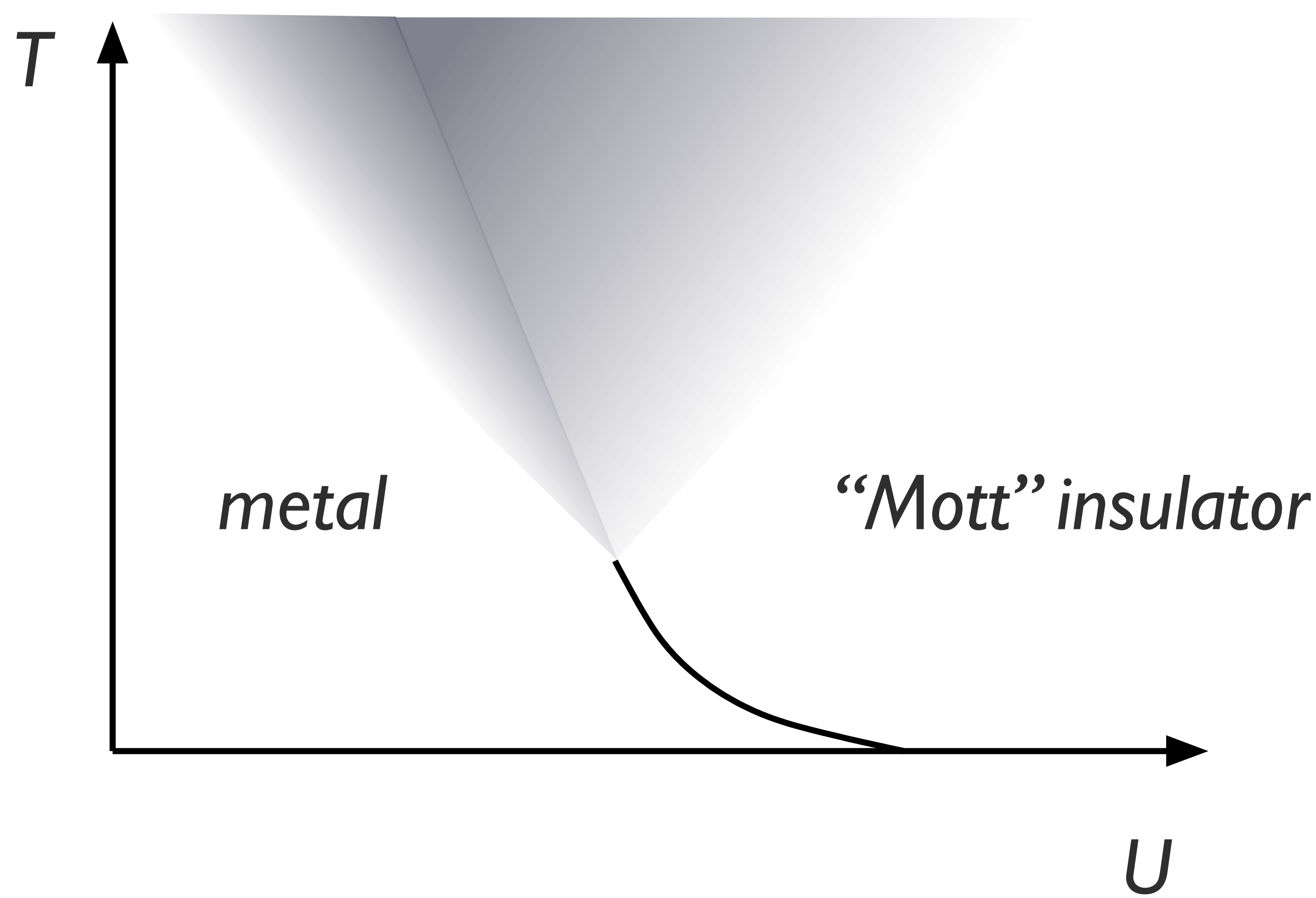

# Model and method

- Equilibrium DMFT phase diagram (half-filling)
- With 2-sublattice order: Antiferromagnetic insulator at low $T$
- Smooth crossover at high $T$

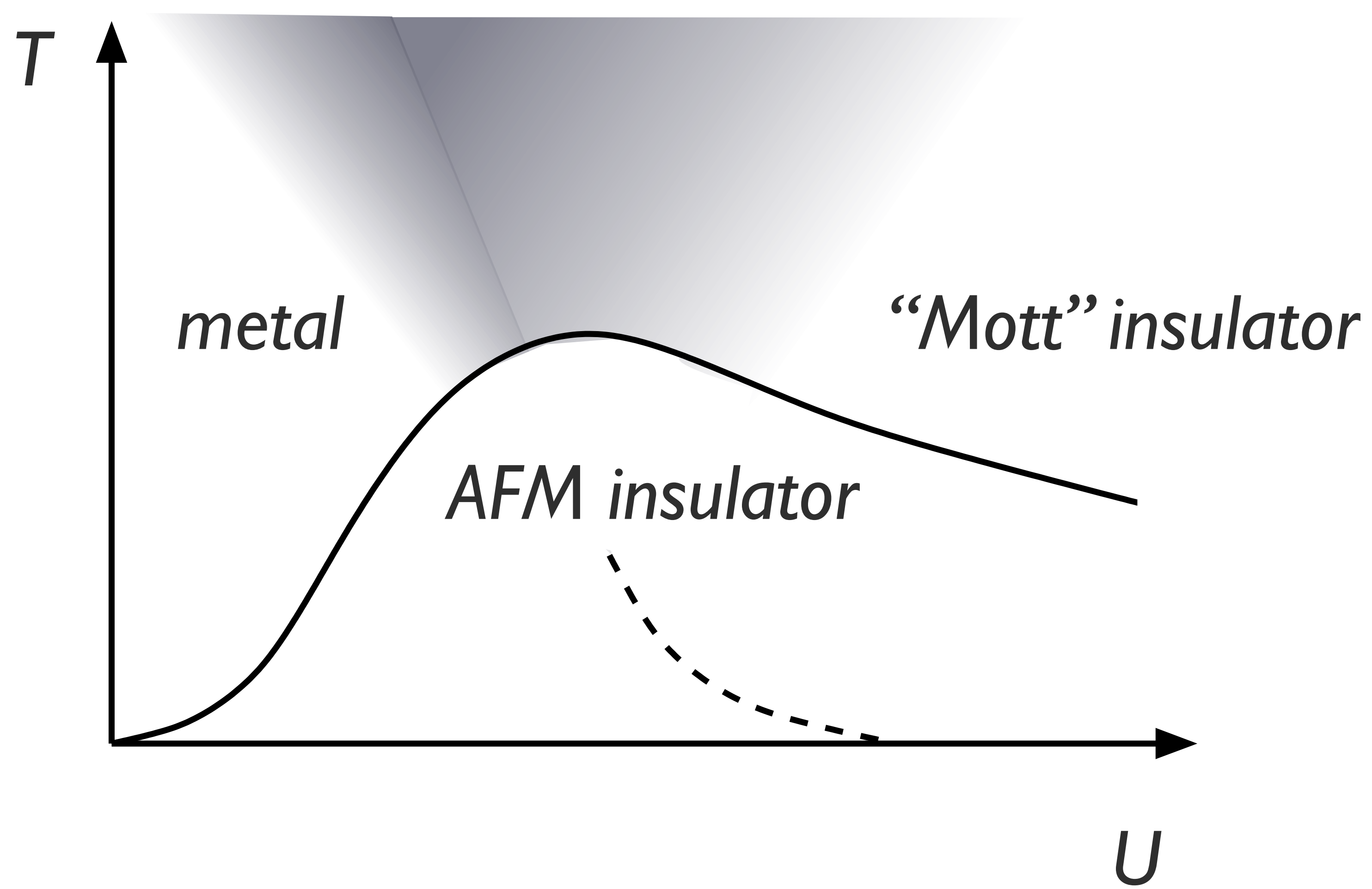

# Model and method

- Equilibrium DMFT phase diagram (half-filling)
- Transformation $c_{i\uparrow} \to c_{i\uparrow}^\dagger \quad (i \in A), \quad c_{i\uparrow} \to -c_{i\uparrow}^\dagger \quad (i \in B)$

  maps repulsive model onto attractive model

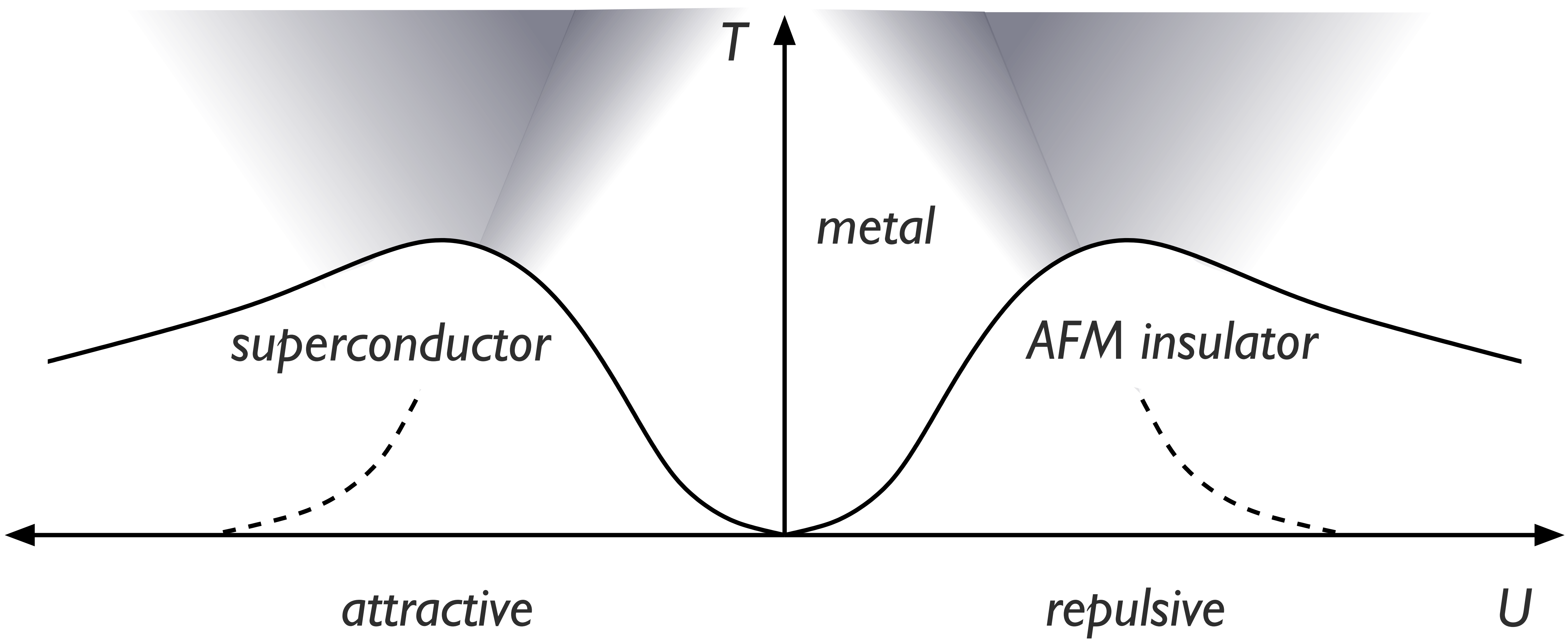

# Model and method

- Equilibrium DMFT phase diagram
- Half-filling: transformation $c_{i\uparrow} \to c_{i\uparrow}^{\dagger} \quad (i \in A), \quad c_{i\uparrow} \to -c_{i\uparrow}^{\dagger} \quad (i \in B)$

  maps repulsive model onto attractive model

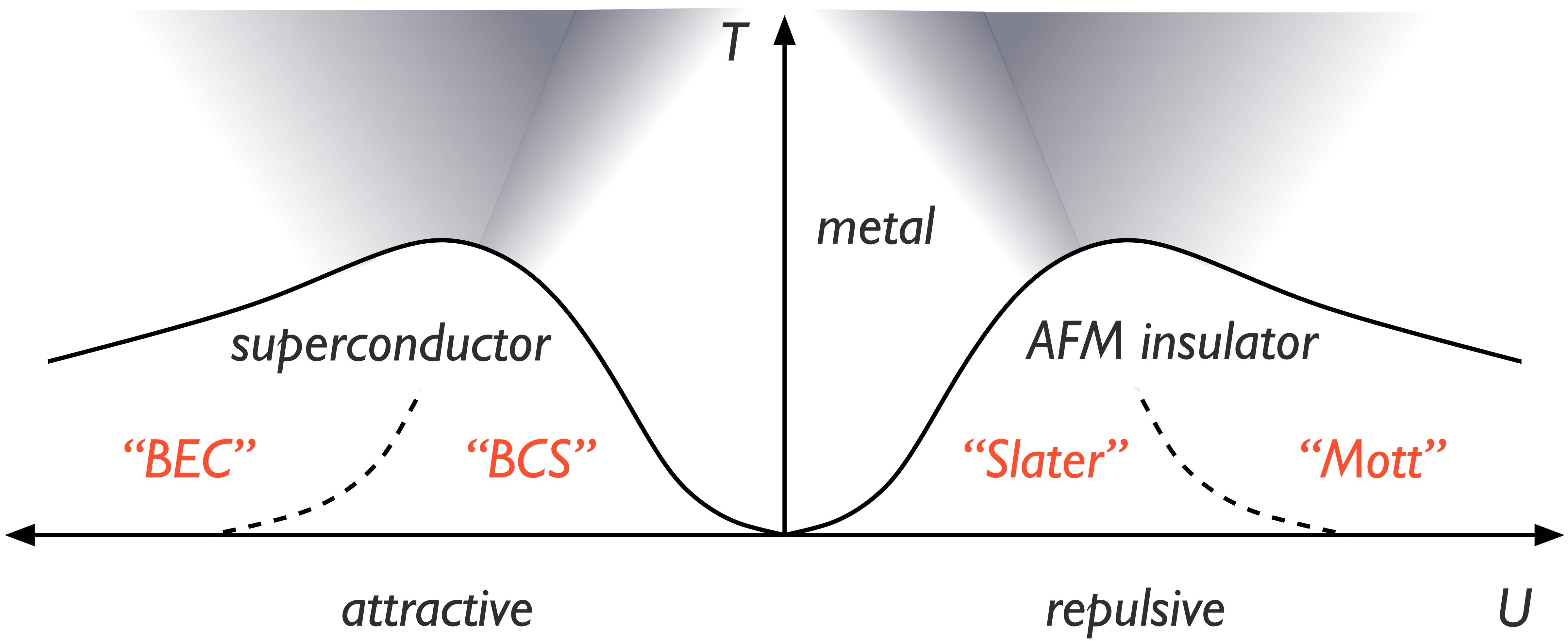

# Nonequilibrium extension

- Kadanoff-Baym contour
- Initial state described by the density matrix $\rho(0) = \frac{1}{Z} e^{-\beta H(0)}$
- State at time *t* described by $\rho(t) = U(t,0)\,\rho(0)\,U(0,t)$

$$U(t,t') = \begin{cases} \mathcal{T} \exp\left(-i \int_{t'}^{t} d\bar{t}\, H(\bar{t})\right) & t > t' \\ \tilde{\mathcal{T}} \exp\left(-i \int_{t'}^{t} d\bar{t}\, H(\bar{t})\right) & t < t' \end{cases}$$

- Time dependent expectation value of observable $\mathcal{O}$

$$\langle \mathcal{O}(t) \rangle = \mathrm{Tr}\left[\rho(t)\mathcal{O}\right] = \mathrm{Tr}\left[U(t,0)\rho(0)U(0,t)\mathcal{O}\right]$$

# Nonequilibrium extension

- Kadanoff-Baym contour
- Express $\rho(0)$ as time-propagation along an imaginary time branch

$$\langle \mathcal{O} \rangle(t) = \mathrm{Tr}\left[\frac{1}{Z}e^{-\beta H(0)} U(0,t)\mathcal{O}U(t,0)\right]$$

$$= \mathrm{Tr}\left[\frac{1}{Z}\left(\mathcal{T}_\tau e^{-\int_0^\beta d\tau H(\tau)}\right)\left(\tilde{\mathcal{T}} e^{i\int_0^t ds H(s)}\right)\mathcal{O}\left(\mathcal{T} e^{-i\int_0^t ds H(s)}\right)\right]$$

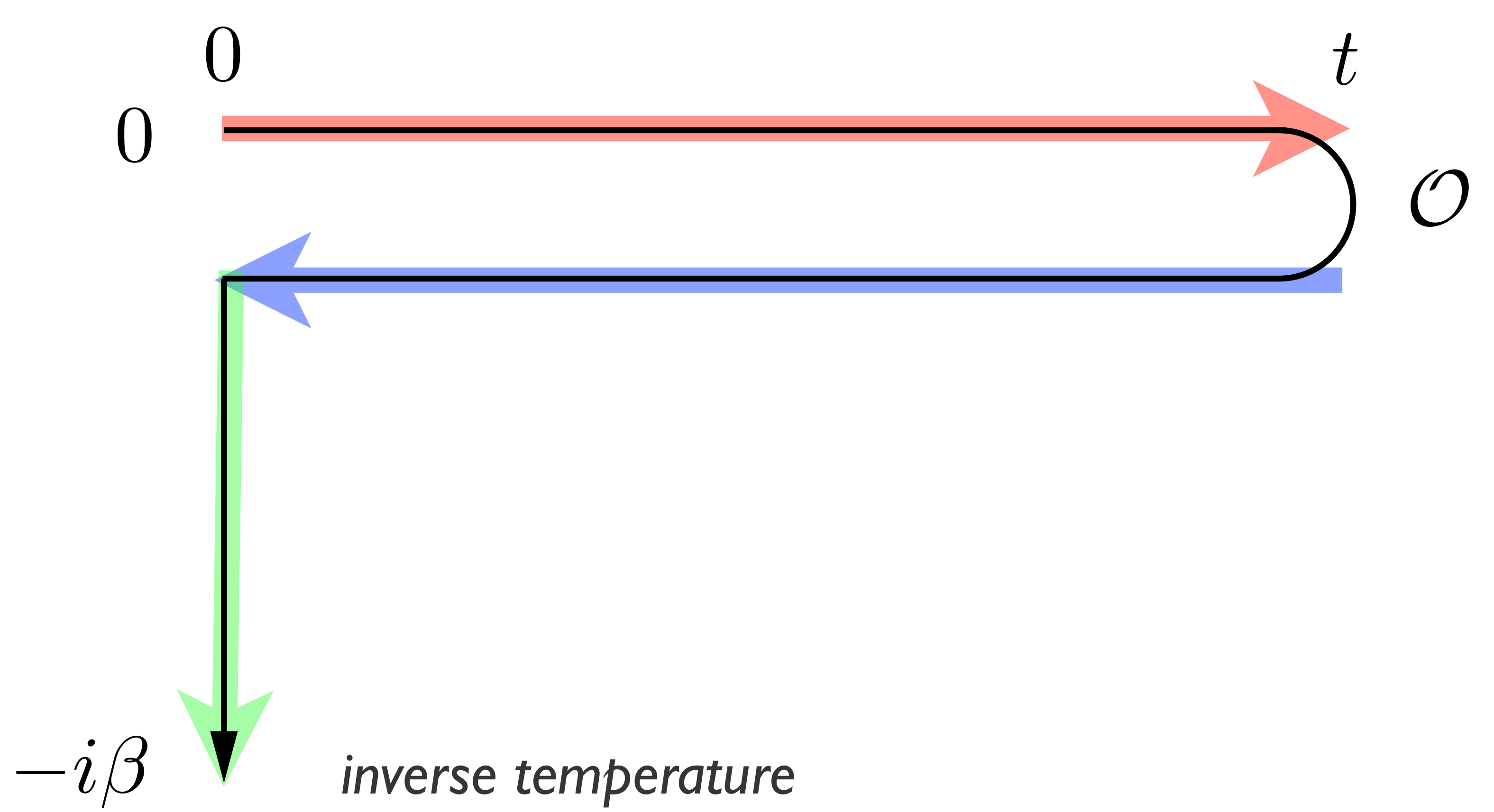

# Nonequilibrium extension

- Kadanoff-Baym contour
- Define contour ordering $\mathcal{T}_\mathcal{C}$ on the contour $\mathcal{C} : 0 \rightarrow t \rightarrow 0 \rightarrow -i\beta$

$$\langle \mathcal{O}(t) \rangle = \frac{1}{Z} \mathrm{Tr}\left[ \mathcal{T}_\mathcal{C}\, e^{-i \int_\mathcal{C} ds\, H(s)} \mathcal{O}(t) \right]$$

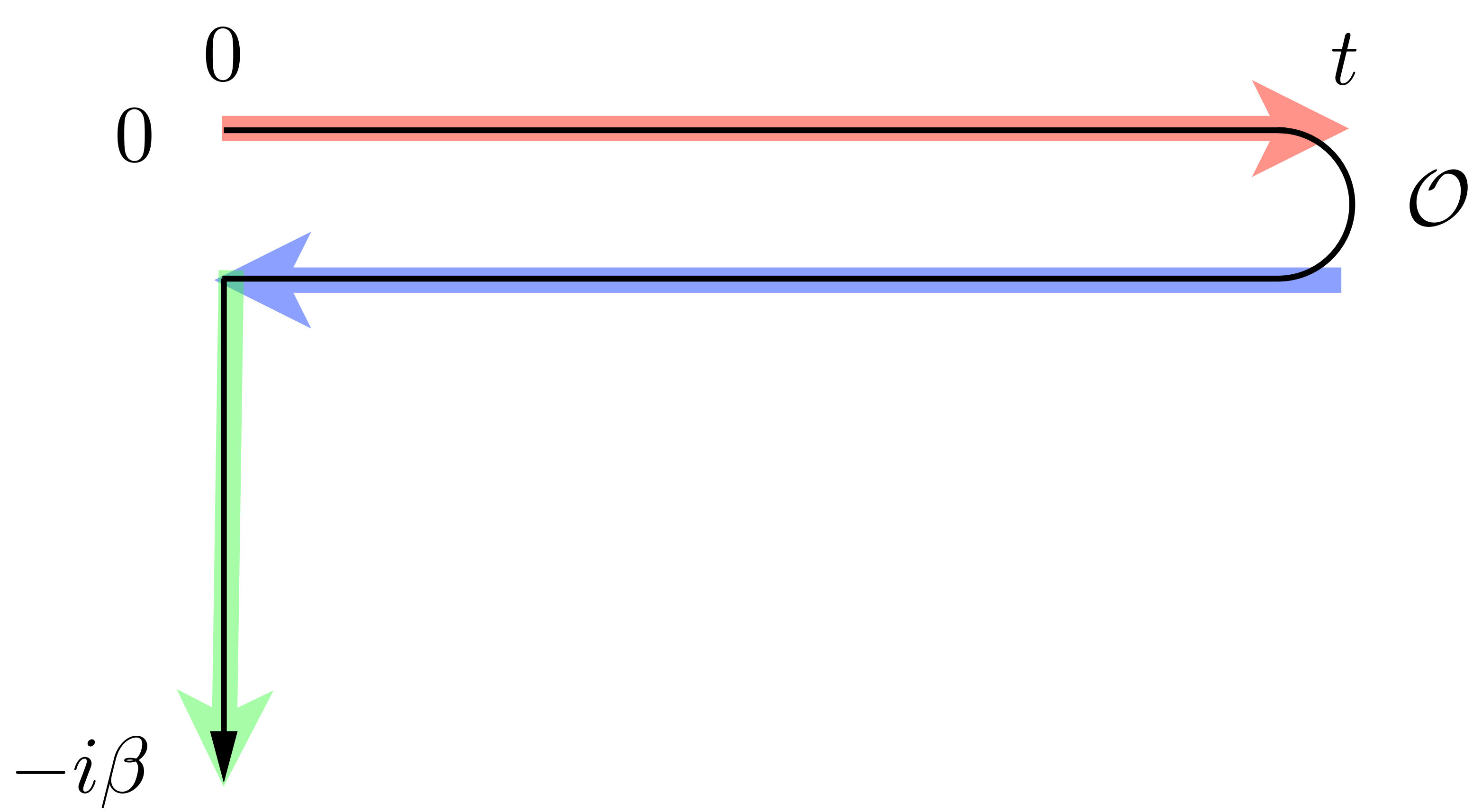

# Nonequilibrium extension

- Kadanoff-Baym contour
- Define contour ordering $\mathcal{T}_\mathcal{C}$ on the contour $\mathcal{C} : 0 \to t \to 0 \to -i\beta$

$$\langle \mathcal{O}(t) \rangle = \frac{1}{Z} \mathrm{Tr}\Big[\mathcal{T}_\mathcal{C}\, e^{-i \int_\mathcal{C} ds\, H(s)} \mathcal{O}(t)\Big]$$

- Contour-ordered formalism can also be applied to 2-point functions

$$\langle \mathcal{T}_\mathcal{C}\, \mathcal{A}(t)\mathcal{B}(t') \rangle \equiv \frac{1}{Z} \mathrm{Tr}\left[\mathcal{T}_\mathcal{C}\, e^{-i \int_\mathcal{C} ds\, H(s)} \mathcal{A}(t)\mathcal{B}(t')\right]$$

- Particularly relevant: Green's function

$$G(t,t') \quad \equiv -i \langle \mathcal{T}_\mathcal{C}\, d(t)\, d^\dagger(t') \rangle$$

# Nonequilibrium extension

- Kadanoff-Baym contour
- Due to the 3 branches, the Green's function has 9 components

$$G(t,t') \equiv G_{ij}(t,t'), \quad t \in \mathcal{C}_i, t' \in \mathcal{C}_j, \quad i,j = 1,2,3$$

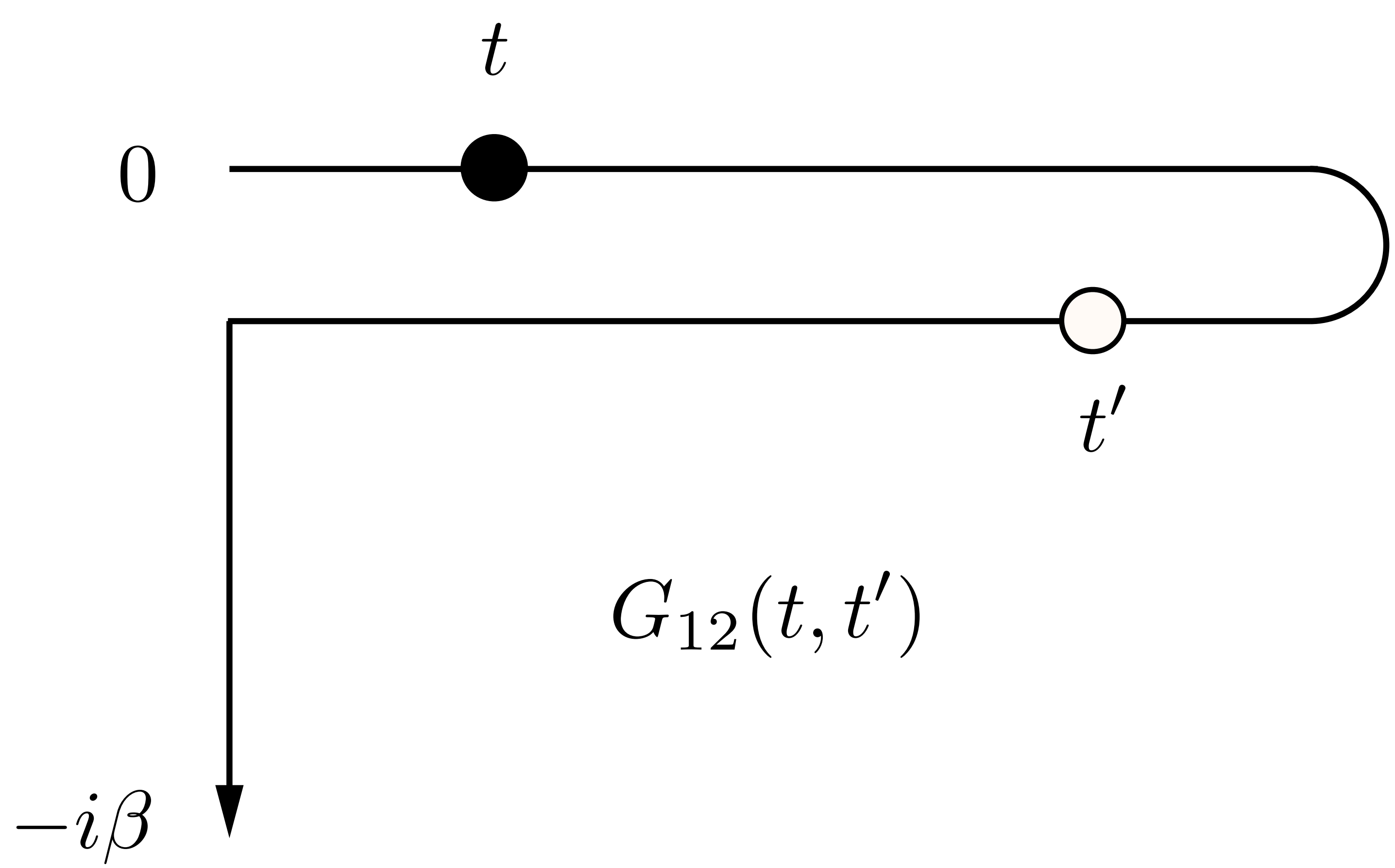

# Nonequilibrium extension

- Kadanoff-Baym contour
- Due to the 3 branches, the Green's function has 9 components

$$G(t,t') \equiv G_{ij}(t,t'), \quad t \in \mathcal{C}_i, t' \in \mathcal{C}_j, \quad i,j = 1,2,3$$

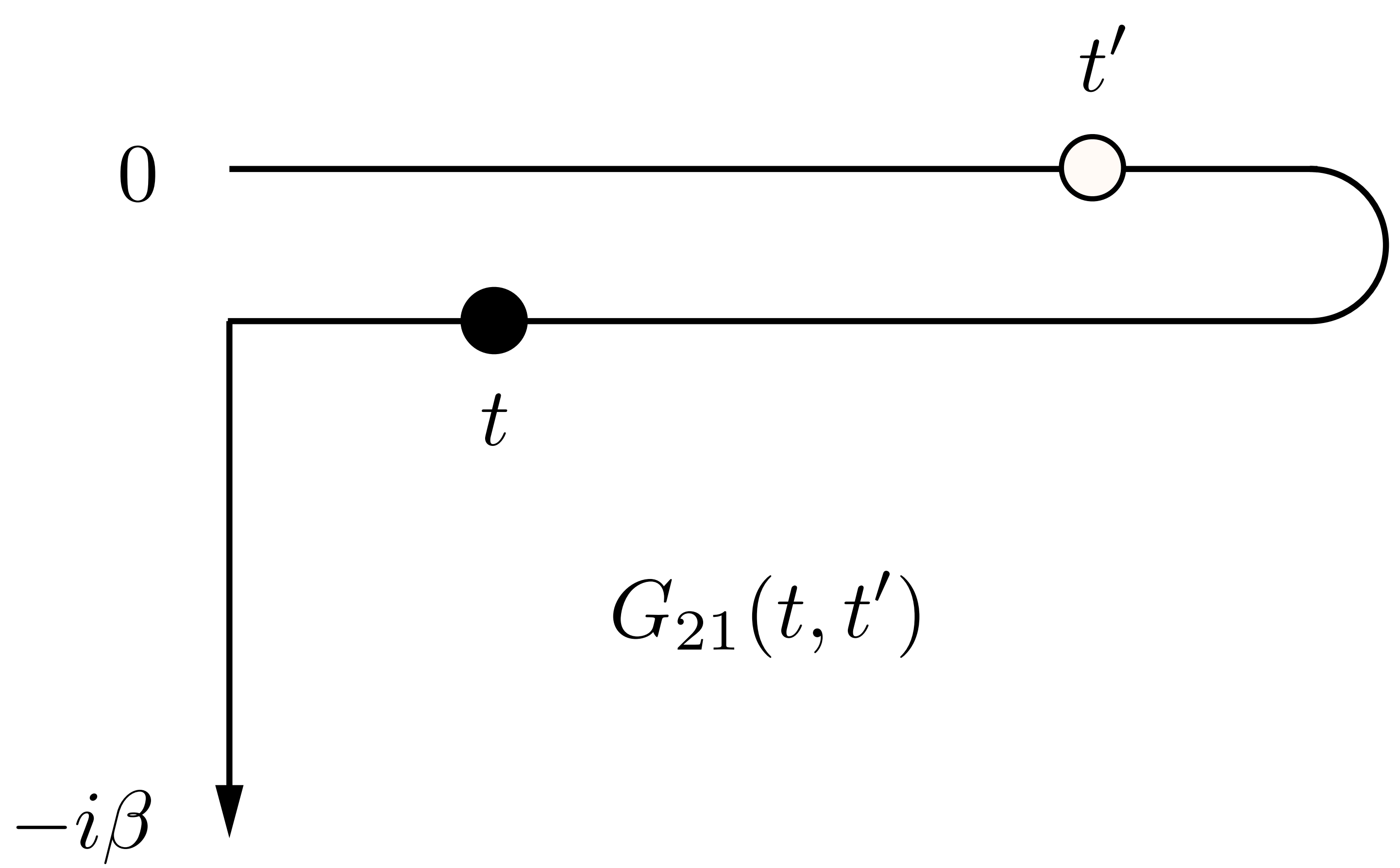

# Nonequilibrium extension

- Kadanoff-Baym contour
- Boundary conditions (cyclic invariance of the trace)

$$G(0_+, t') = -G(-i\beta, t')$$

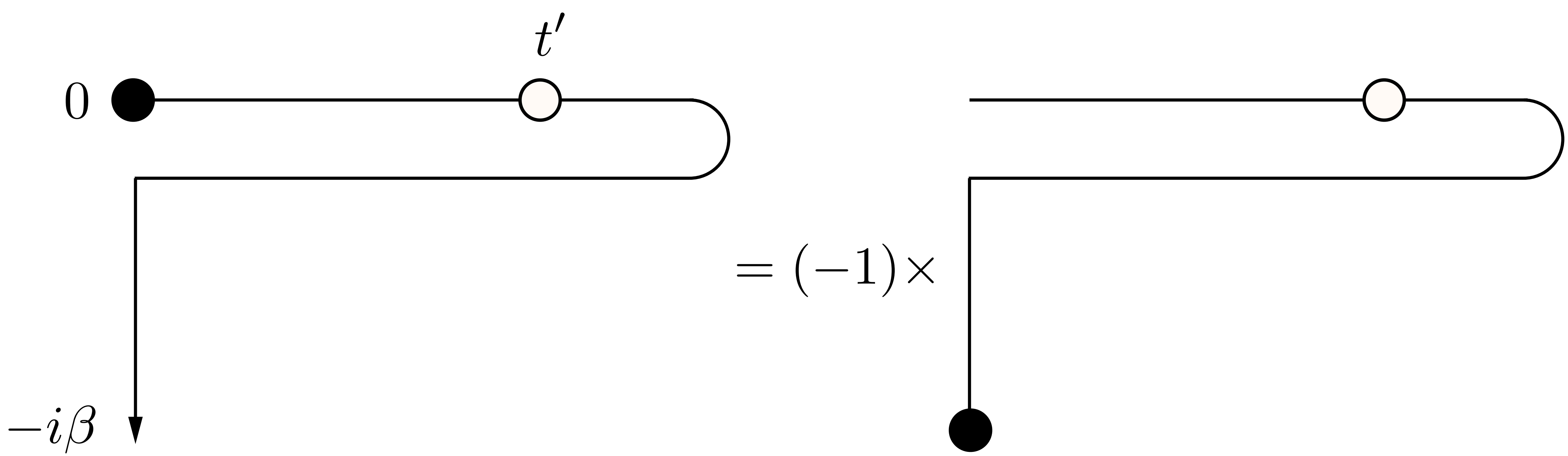

# Nonequilibrium extension

- Kadanoff-Baym contour
- Boundary conditions (cyclic invariance of the trace)

$$G(0_+, t') = -G(-i\beta, t')$$

$$G(t, 0_+) = -G(t, -i\beta)$$

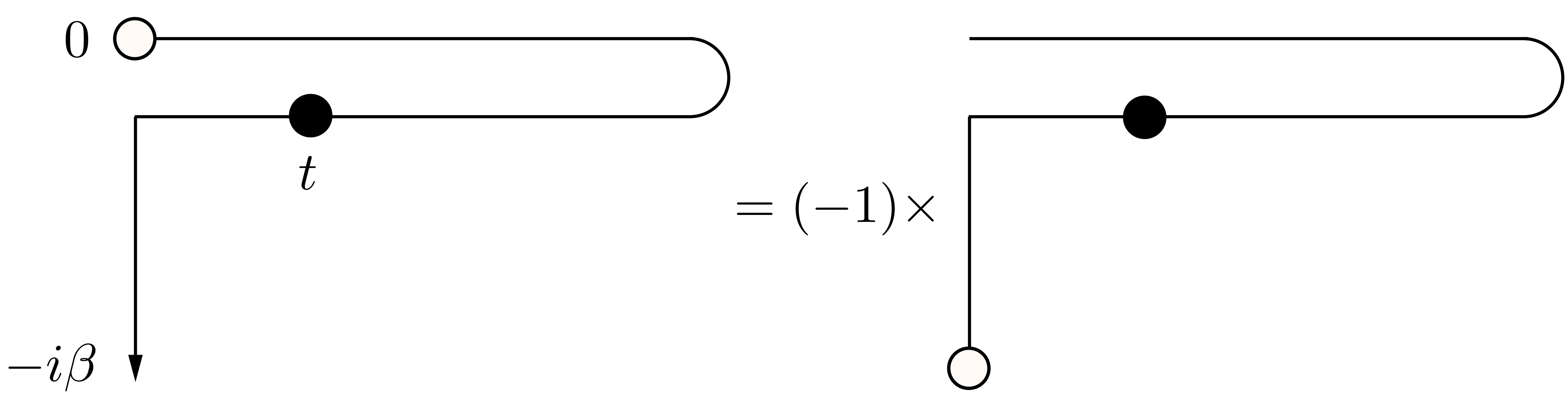

# Nonequilibrium extension

- Nonequilibrium DMFT: Solve DMFT equations on the Kadanoff-Baym contour $\mathcal{C}$ *Freericks et al. (2006)*

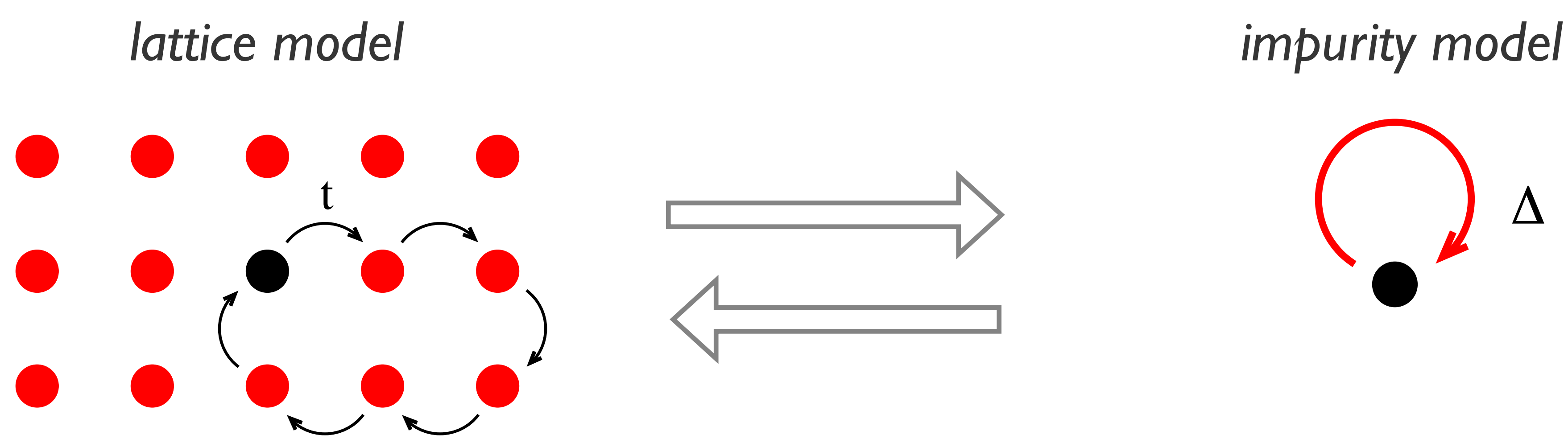


*DMFT self-consistency*

$$G_{\mathrm{loc}}^{\mathrm{latt}}(t,t') \quad \Longrightarrow \quad S_{\mathrm{imp}}[\Delta(t,t')]$$

$$G_{\mathrm{loc}}^{\mathrm{latt}} \equiv G_{\mathrm{imp}}$$

*momentum average* $\Uparrow$ $\qquad$ $\Downarrow$ *impurity solver*

$$\Sigma_k^{\mathrm{latt}} \equiv \Sigma_{\mathrm{imp}}$$

$$G_k^{\mathrm{latt}} = \frac{1}{i\partial_t + \mu - \epsilon_k - \Sigma_k^{\mathrm{latt}}} \quad \Longleftarrow \quad G_{\mathrm{imp}}(t,t'), \Sigma_{\mathrm{imp}}(t,t')$$

*DMFT approximation*

# Nonequilibrium extension

- Nonequilibrium DMFT: Solve DMFT equations on the Kadanoff-Baym contour $\mathcal{C}$
- Nonequilibrium Anderson impurity model

$$S_{\mathrm{imp}} = -i \int_{\mathcal{C}} dt\, H_{\mathrm{loc}}(t) - i \sum_{\sigma} \int_{\mathcal{C}} dt\, dt'\, d_{\sigma}^{\dagger}(t) \Delta(t, t') d_{\sigma}(t')$$

*interaction and chemical potential terms* *contour hybridization function*

- Impurity Green's function

$$G_{\mathrm{imp}}(t, t') = -i \langle \mathcal{T}_{\mathcal{C}}\, d(t) d^{\dagger}(t') \rangle_{S_{\mathrm{imp}}}$$

$$\langle \cdots \rangle_{S_{\mathrm{imp}}} = \frac{\mathrm{Tr}[\mathcal{T}_{\mathcal{C}}\ \exp(S_{\mathrm{imp}}) \cdots]}{\mathrm{Tr}[\mathcal{T}_{\mathcal{C}}\ \exp(S_{\mathrm{imp}})]}$$

# Nonequilibrium extension

- Calculation of the lattice Green's function
- Noninteracting lattice:

$$H_0(t) = \sum_k [\epsilon_k(t) - \mu(t)] d_k^\dagger d_k$$

$$G_{0,k}(t,t') = -i\langle \mathcal{T}_\mathcal{C} d_k(t) d_k^\dagger(t')\rangle_0$$

- Green's function satisfies:

$$\begin{aligned} \big[i\partial_t + \mu(t) - \epsilon_k(t)\big] G_{0,k}(t,t') &= \delta_\mathcal{C}(t,t') \\ G_{0,k}(t,t')\big[-i\overleftarrow{\partial}_{t'} + \mu(t') - \epsilon_k(t')\big] &= \delta_\mathcal{C}(t,t') \end{aligned}$$

- Inverse lattice Green's function:

$$G_{0,k}^{-1}(t,t') = \big[i\partial_t + \mu(t) - \epsilon_k(t)\big]\delta_\mathcal{C}(t,t')$$

# Nonequilibrium extension

- Calculation of the lattice Green's function
- Interacting lattice Green's function satisfies Dyson equation:

$$\begin{aligned} G_k &= G_{0,k} + G_{0,k} \star \Sigma \star G_k \\ &= G_{0,k} + G_k \star \Sigma \star G_{0,k} \end{aligned}$$

*integral form*

$\Uparrow$

*impurity self-energy (DMFT)*

$$[G_{0,k}^{-1} - \Sigma] \star G_k = G_k \star [G_{0,k}^{-1} - \Sigma] = \delta_{\mathcal{C}}$$

*differential form*

- Imaginary-time branch: boundary-value problem $\longrightarrow$ solve by FT

$$G_k(i\omega_n) = \frac{1}{G_{0,k}^{-1}(i\omega_n) - \Sigma(i\omega_n)} = \frac{1}{i\omega_n + \mu(0) - \epsilon_k(0) - \Sigma(i\omega_n)}$$

- Usual equilibrium DMFT calculation for the initial equilibrium state

# Nonequilibrium extension

- Calculation of the lattice Green's function

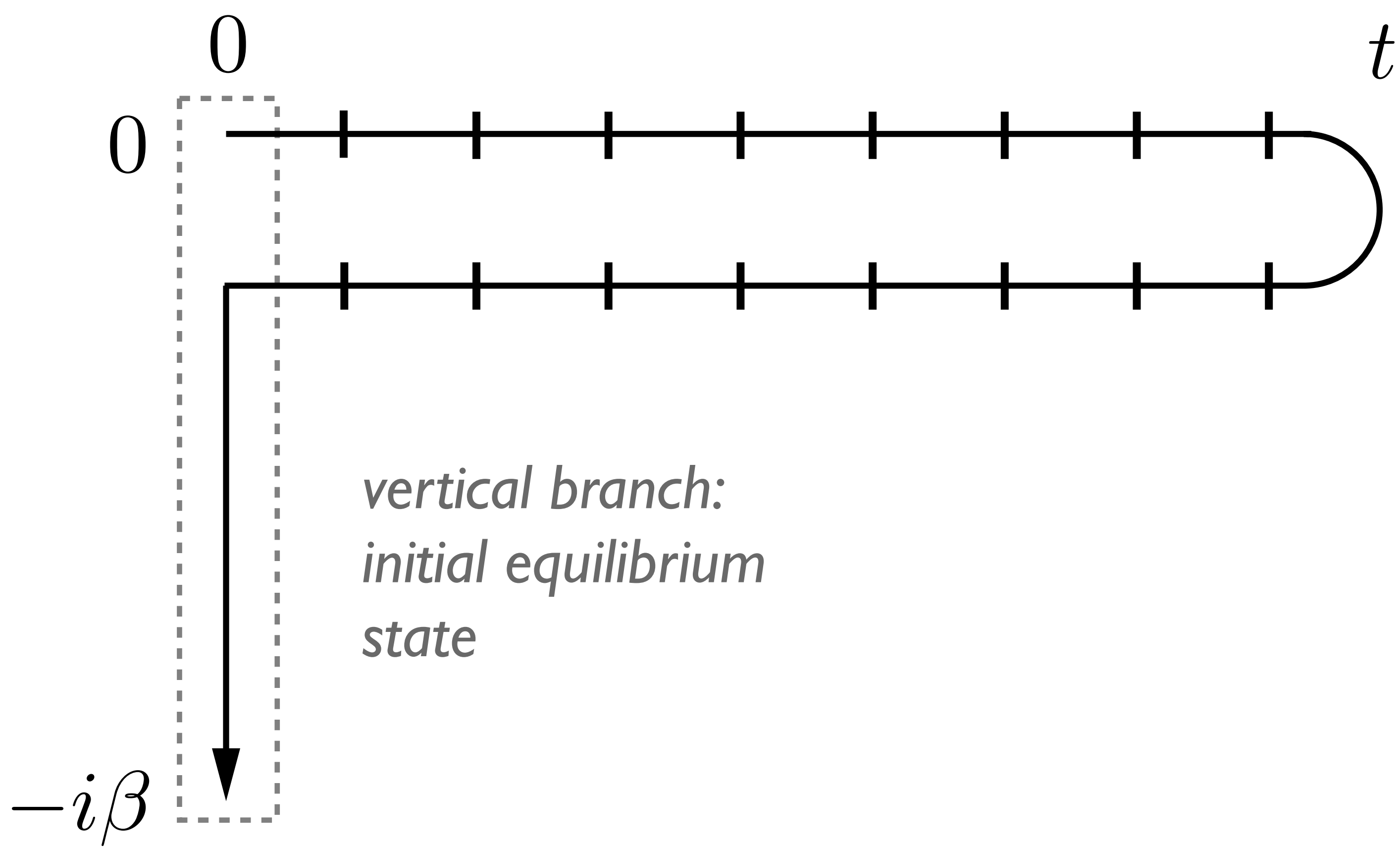


*vertical branch: initial equilibrium state*

*propagate and converge the DMFT solution step by step along the real-time axis*

- Real-time branches: initial-value problem

$$[i\partial_t + \mu(t) - \epsilon_k(t)]G_k(t,t') - \int_{\mathcal{C}} d\bar{t}\, \Sigma(t,\bar{t})G_k(\bar{t},t') = \delta_{\mathcal{C}}(t,t')$$

- Defines time-propagation scheme for G in which the self-energy plays the role of a memory-kernel

# Nonequilibrium extension

- Electric fields
- Vector potential $A(r,t)$, scalar potential $\Phi(r,t)$: $E = -\nabla\Phi - \partial_t A$

$$v_{ij}(t) = v_{ij}\exp\Big(-ie\int_{R_i}^{R_j} dr\, A(r,t)\Big)$$

$$\Downarrow$$

$$H(t) = -\sum_{\langle ij\rangle\sigma} v_{ij}(t)(d^\dagger_{i\sigma}d_{j\sigma} + d^\dagger_{j\sigma}d_{i\sigma}) + U(t)\sum_i n_{i\uparrow}n_{i\downarrow} - \sum_{i\sigma}\mu_i(t)n_{i\sigma}$$

$$\Uparrow$$

$$\mu_i(t) = \mu + e\Phi(t)(R_i,t)$$

- Convenient choice: gauge with pure vector potential:

  $\Phi \equiv 0, E = -\partial_t A$

# Nonequilibrium extension

- Electric fields
- Neglecting the *r*-dependence of *A* (assumption: field varies slowly on the atomic scale):

$$v_{ij}(t) = v_{ij} \exp\left(-ie\int_{R_i}^{R_j} dr\, A(t)\right) \qquad A(t) = -\int_0^t ds E(s)$$

$$\Big\Downarrow \quad \textit{Fourier transformation}$$

$$\boxed{\epsilon_k(t) = \epsilon_{k-eA(t)}}$$

- Electric field enters in the lattice Dyson equation in the form of a time-dependent dispersion:

$$[i\partial_t + \mu(t) - \epsilon_k(t)]G_k(t,t') - \int_{\mathcal{C}} d\bar{t}\,\Sigma(t,\bar{t})G_k(\bar{t},t') = \delta_{\mathcal{C}}(t,t')$$

# Spectroscopy

- "Physical" Green's functions
- The 9 elements of the 3x3 Green's function matrix

$$\hat{G} = \begin{pmatrix} G_{11} & G_{12} & G_{13} \\ G_{21} & G_{22} & G_{23} \\ G_{31} & G_{32} & G_{33} \end{pmatrix}$$

are not independent:

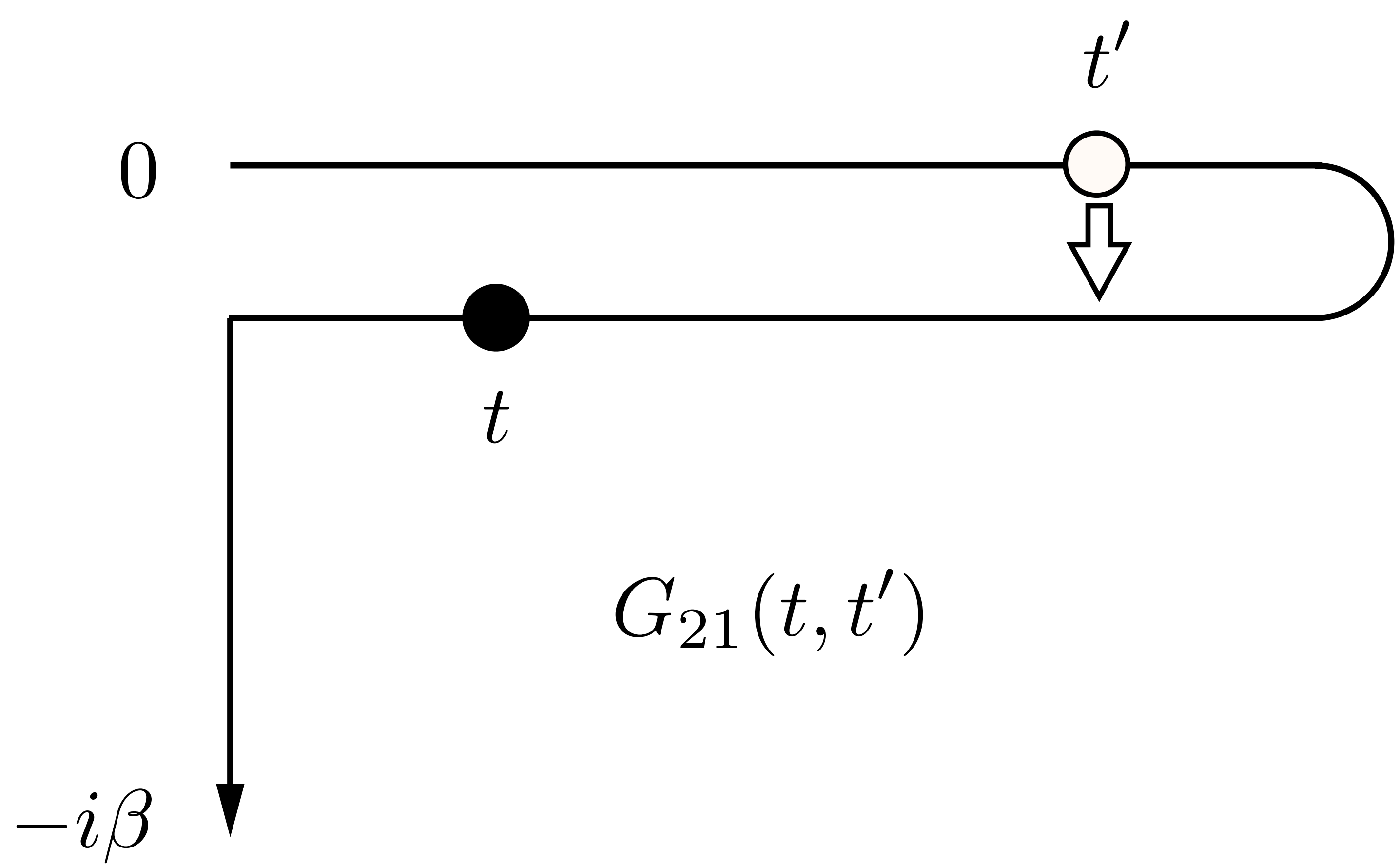

# Spectroscopy

- "Physical" Green's functions
- The 9 elements of the 3x3 Green's function matrix

$$\hat{G} = \begin{pmatrix} G_{11} & G_{12} & G_{13} \\ G_{21} & G_{22} & G_{23} \\ G_{31} & G_{32} & G_{33} \end{pmatrix}$$

are not independent:

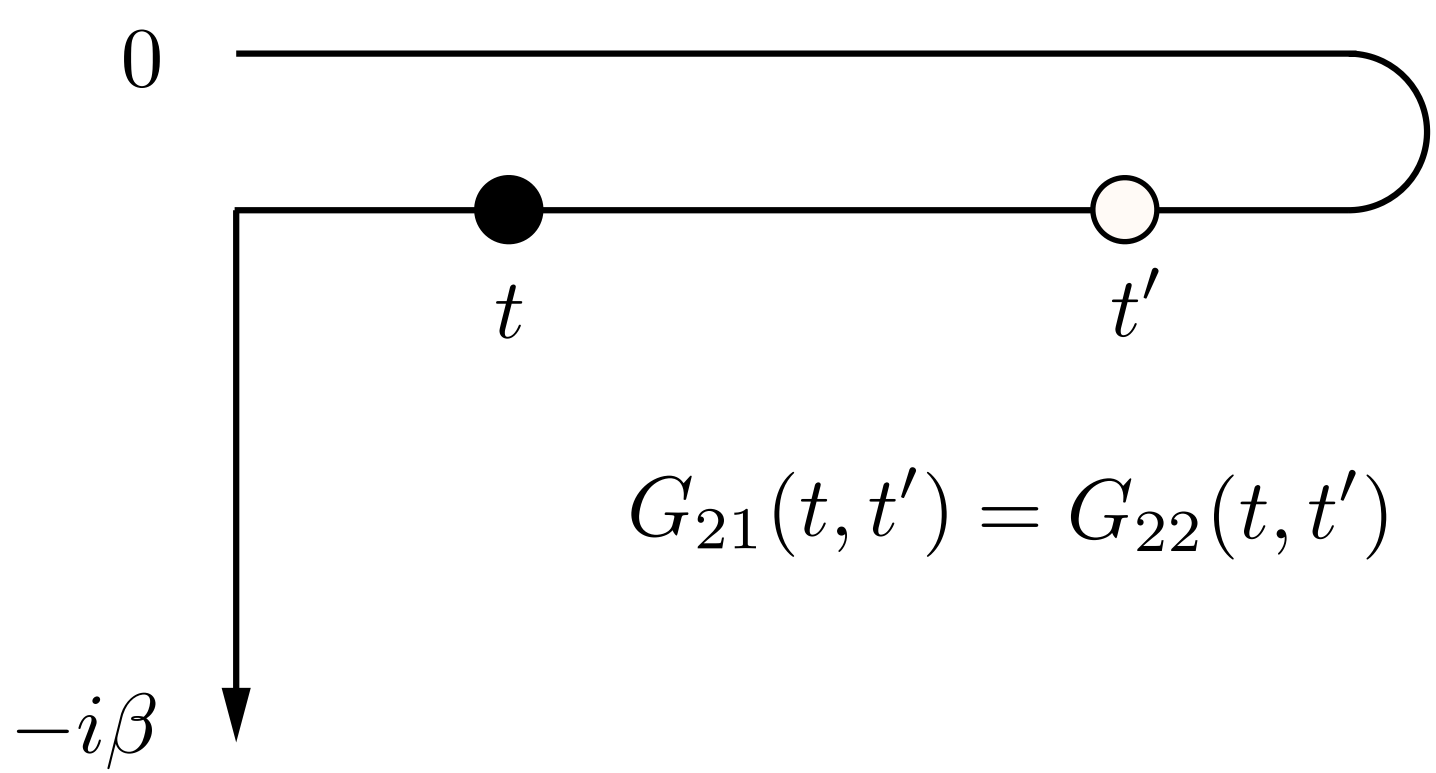


$$G_{21}(t, t') = G_{22}(t, t') \quad (\text{for } t < t')$$

# Spectroscopy

- "Physical" Green's functions
- We have the following redundancies

$$
\begin{aligned}
G_{11}(t,t') &= G_{12}(t,t') \quad (\text{for } t \le t') \\
G_{11}(t,t') &= G_{21}(t,t') \quad (\text{for } t > t') \\
G_{22}(t,t') &= G_{21}(t,t') \quad (\text{for } t < t') \\
G_{22}(t,t') &= G_{12}(t,t') \quad (\text{for } t \ge t') \\
G_{13}(t,\tau') &= G_{23}(t,\tau') \\
G_{31}(\tau,t') &= G_{32}(\tau,t')
\end{aligned}
$$

which allow to eliminate 3 of the 9 components

$\longrightarrow$ define 6 "physical" Green's functions

$$G^R, G^A, G^K, \ldots$$

# Spectroscopy

- "Physical" Green's functions
- Relevant for the following discussion: Retarded Green's function

$$G^R(t,t') = \tfrac{1}{2}(G_{11} - G_{12} + G_{21} - G_{22}) = -i\theta(t-t')\langle\{d(t), d^\dagger(t')\}\rangle$$

and lesser Green's functions

$$G^<(t,t') = G_{12} = i\langle d^\dagger(t')d(t)\rangle$$

- In equilibrium:
  - Spectral function: $A(\omega) = -\frac{1}{\pi}\mathrm{Im}\, G^R(\omega)$
  - Occupation: $N(\omega) = \frac{1}{2\pi}\mathrm{Im}\, G^<(\omega)$
  - Distribution function: $N(\omega)/A(\omega) = f(\omega)$ *Fermi function*

# Spectroscopy

- "Physical" Green's functions
- Relevant for the following discussion: Retarded Green's function

$$G^R(t,t') = \tfrac{1}{2}(G_{11} - G_{12} + G_{21} - G_{22}) = -i\theta(t-t')\langle\{d(t), d^\dagger(t')\}\rangle$$

and lesser Green's functions

$$G^<(t,t') = G_{12} = i\langle d^\dagger(t')d(t)\rangle$$

- Out of equilibrium: $t_{\text{av}} = (t+t')/2, t_{\text{rel}} = t - t'$
  - Spectral function: $A(\omega, t_{\text{av}}) = -\frac{1}{\pi}\text{Im}\int dt_{\text{rel}} e^{i\omega t_{\text{rel}}} G^R(t,t')$
  - Occupation: $N(\omega, t_{\text{av}}) = \frac{1}{2\pi}\text{Im}\int dt_{\text{rel}} e^{i\omega t_{\text{rel}}} G^<(t,t')$
  - "Distribution function": $N(\omega, t_{\text{av}})/A(\omega, t_{\text{av}})$

# Spectroscopy

- Time-resolved photoemission spectrum

$$\cos[\Omega(t - t_p + \phi)]S(t - t_p)$$

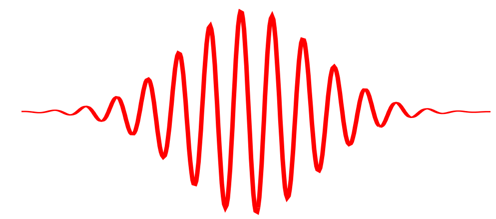

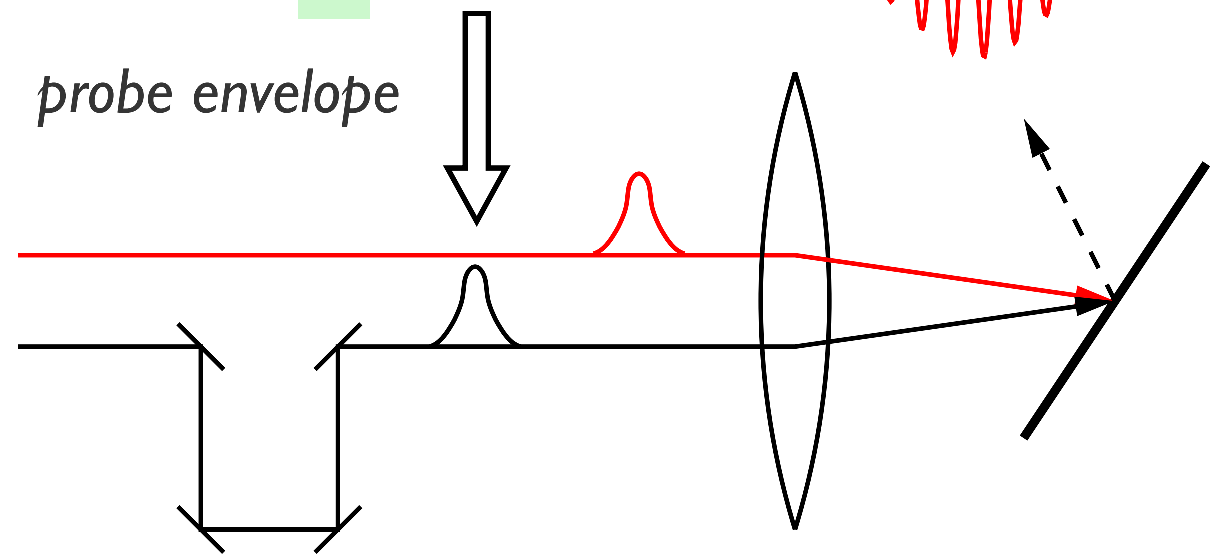


$$I(k_f, E; t_p) \propto \sum_k \delta_{k_\| + q_\|, k_{f\|}} I_k(E - \hbar\Omega_q - W; t_p),$$

$$I_k(\omega; t_p) = -i \int dt dt' \, S(t) S(t') e^{i\omega(t'-t)} G_k^<(t + t_p, t' + t_p)$$

probe time

# Spectroscopy

- Time-resolved photoemission spectrum

$$\cos[\Omega(t - t_p + \phi)]S(t - t_p)$$

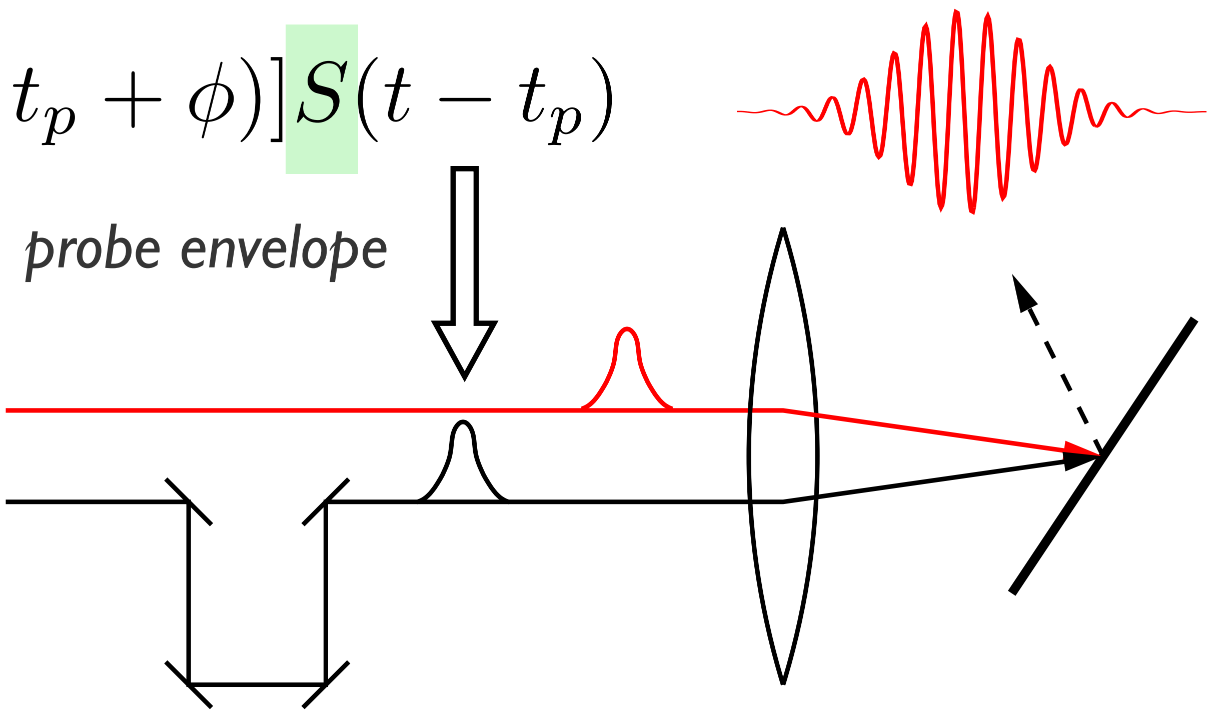


$$S(t) \sim \delta(t - t_p) : \text{ measure occupation } n_k(t_p)$$

$$S(t) \sim \text{const} : \text{ measure spectral function } A_k(\omega, t_p)$$

$$I_k(\omega; t_p) = -i \int dt dt' \, S(t) S(t') e^{i\omega(t'-t)} G_k^<(t + t_p, t' + t_p)$$

- Formula contains time-energy uncertainty

# 1. Periodic electric fields

- AC-field quench in the Hubbard model (metal phase)

  *Tsuji, Oka, Werner & Aoki, PRL 106, 236401 (2011)*

Electric field (amplitude *E*, frequency $\Omega$)
applied at *t*=0

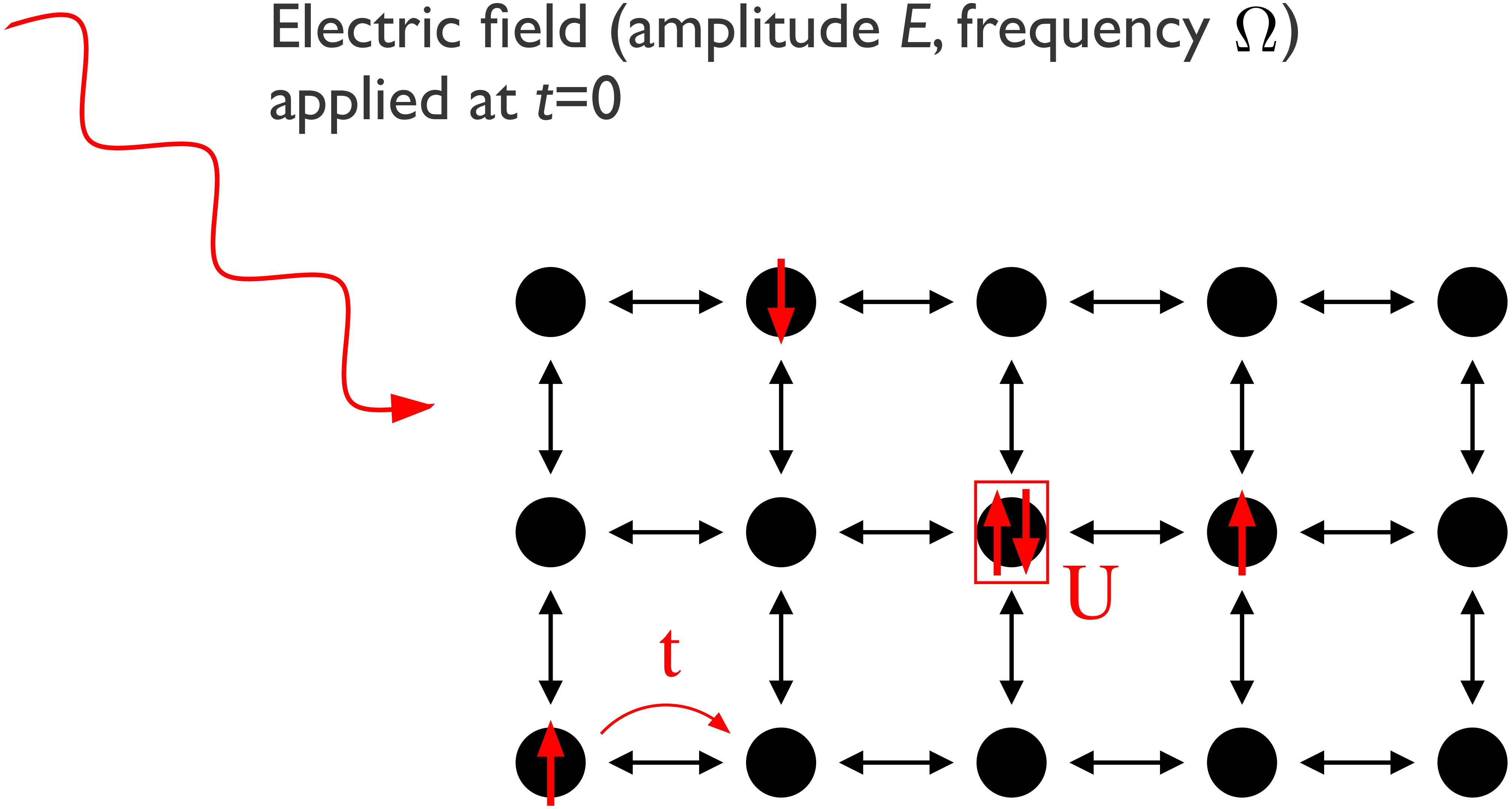

# 1. Periodic electric fields

- AC-field quench in the Hubbard model (metal phase)

*Tsuji, Oka, Werner & Aoki, PRL 106, 236401 (2011)*

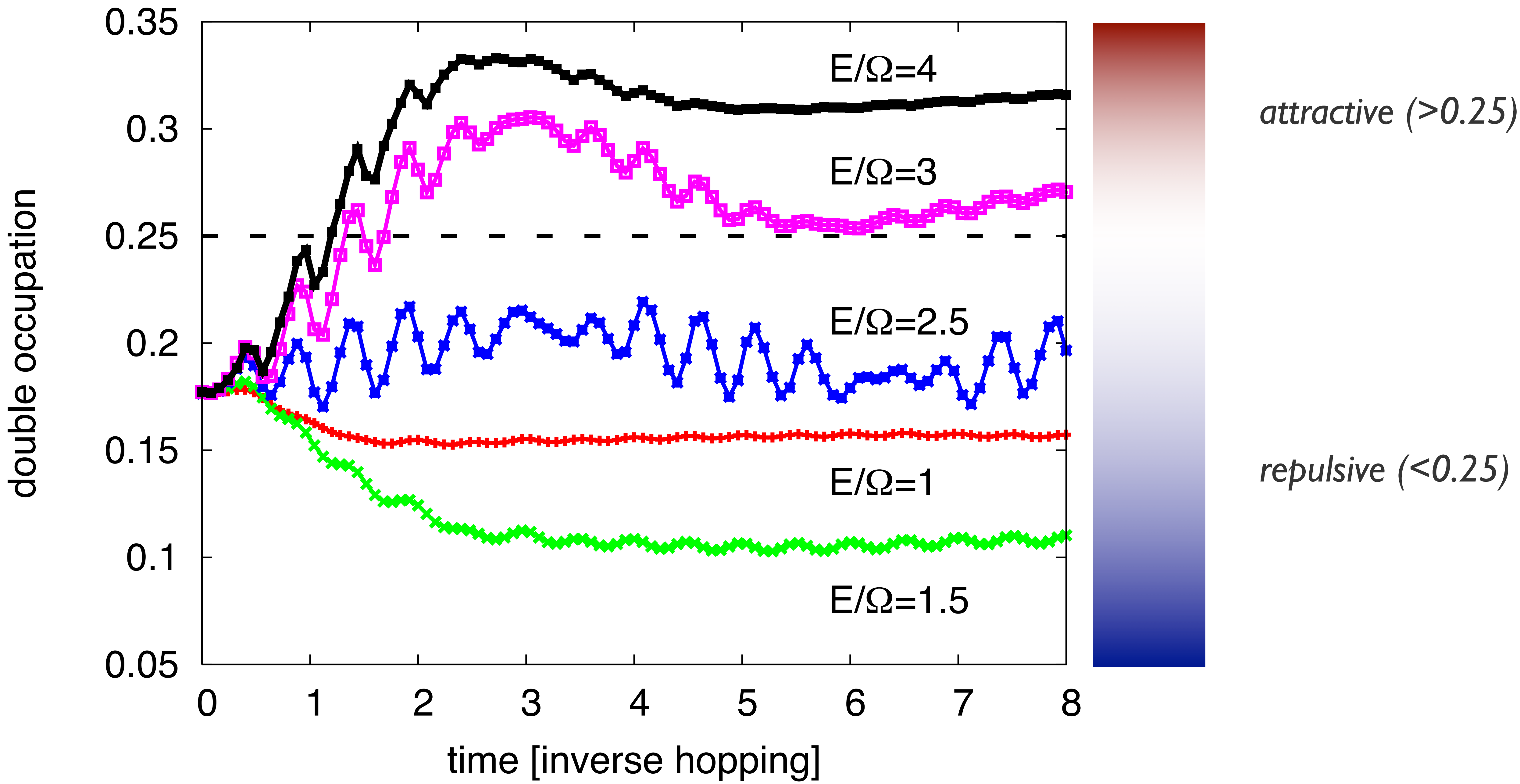

# 1. Periodic electric fields

- AC-field quench in the Hubbard model (metal phase)
  - Sign inversion of the interaction: repulsive ↔ attractive
  - *Dynamically generated* high-Tc superconductivity?

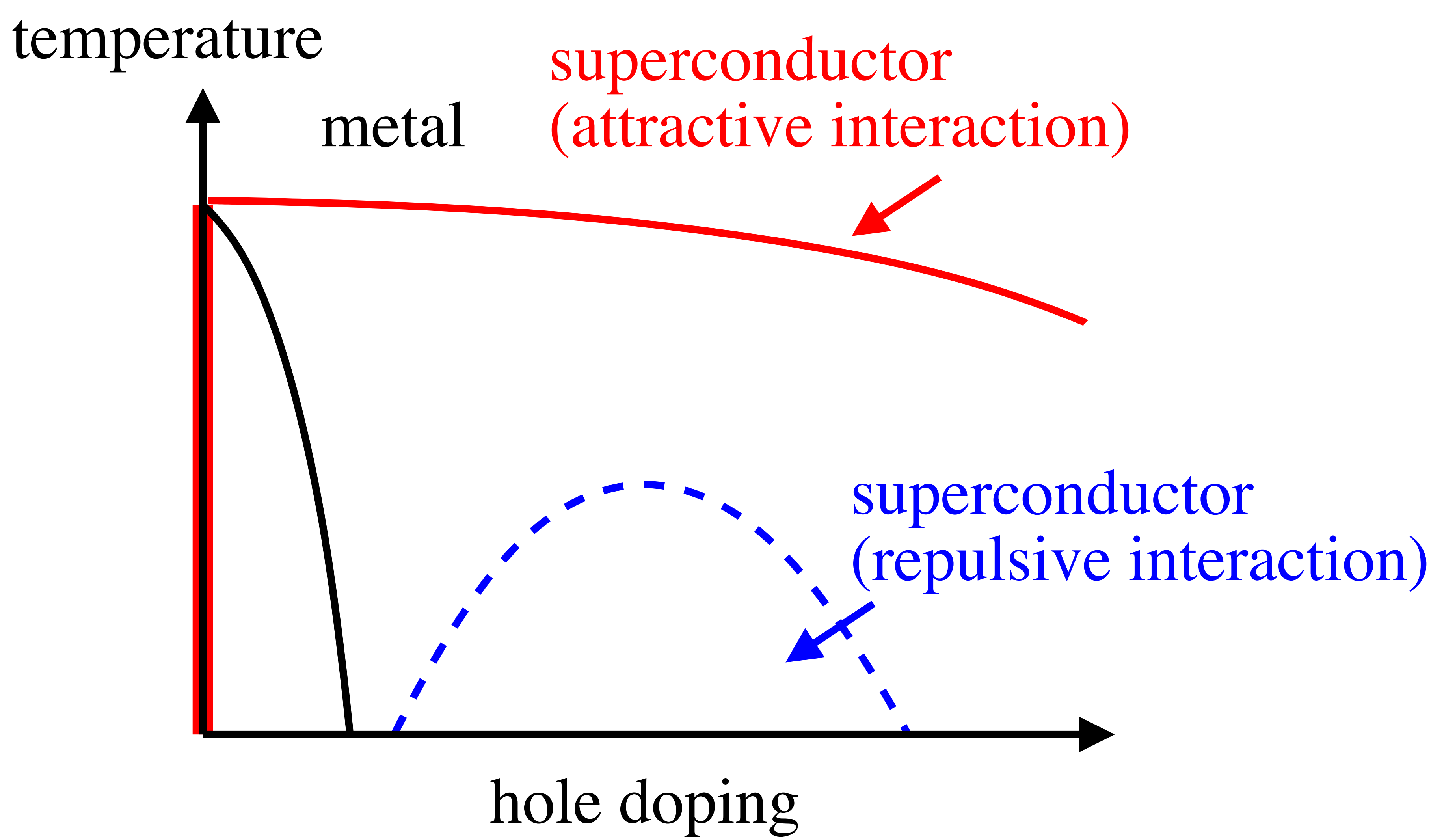

# I. Origin of the attractive interaction

- Periodic E-field leads to a population inversion

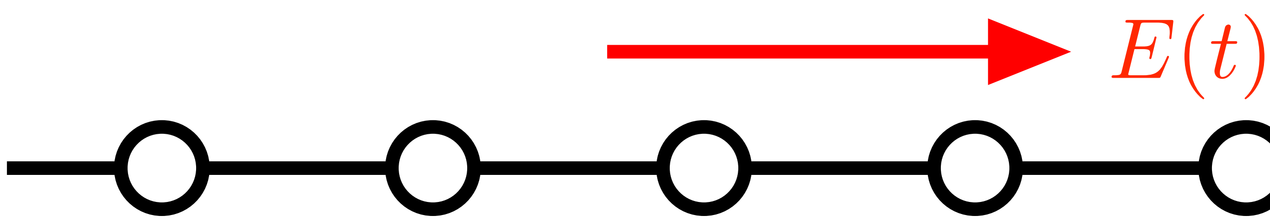


- Gauge with pure vector potential

$$E(t) = E\cos(\Omega t) = -\partial_t A(t)$$
$$\Rightarrow A(t) = -(E/\Omega)\sin(\Omega t)$$

- Peierls substitution $\epsilon_k \longrightarrow \epsilon_{k-A(t)}$

- Renormalized dispersion

$$\overline{\epsilon_k} = \frac{\Omega}{2\pi}\int_0^{2\pi/\Omega} dt\,\epsilon_{k-A(t)} = \mathcal{J}_0(E/\Omega)\epsilon_k$$

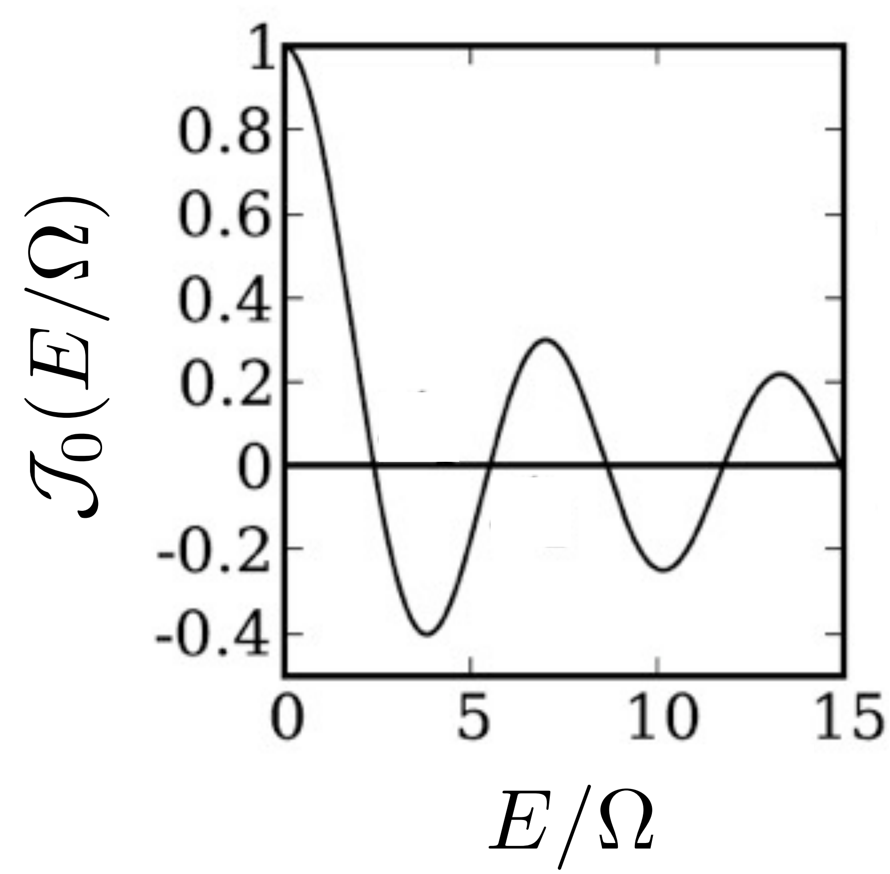

# I. Origin of the attractive interaction

- Periodic E-field leads to a population inversion

$$\mathcal{J}_0(E/\Omega) = 1$$

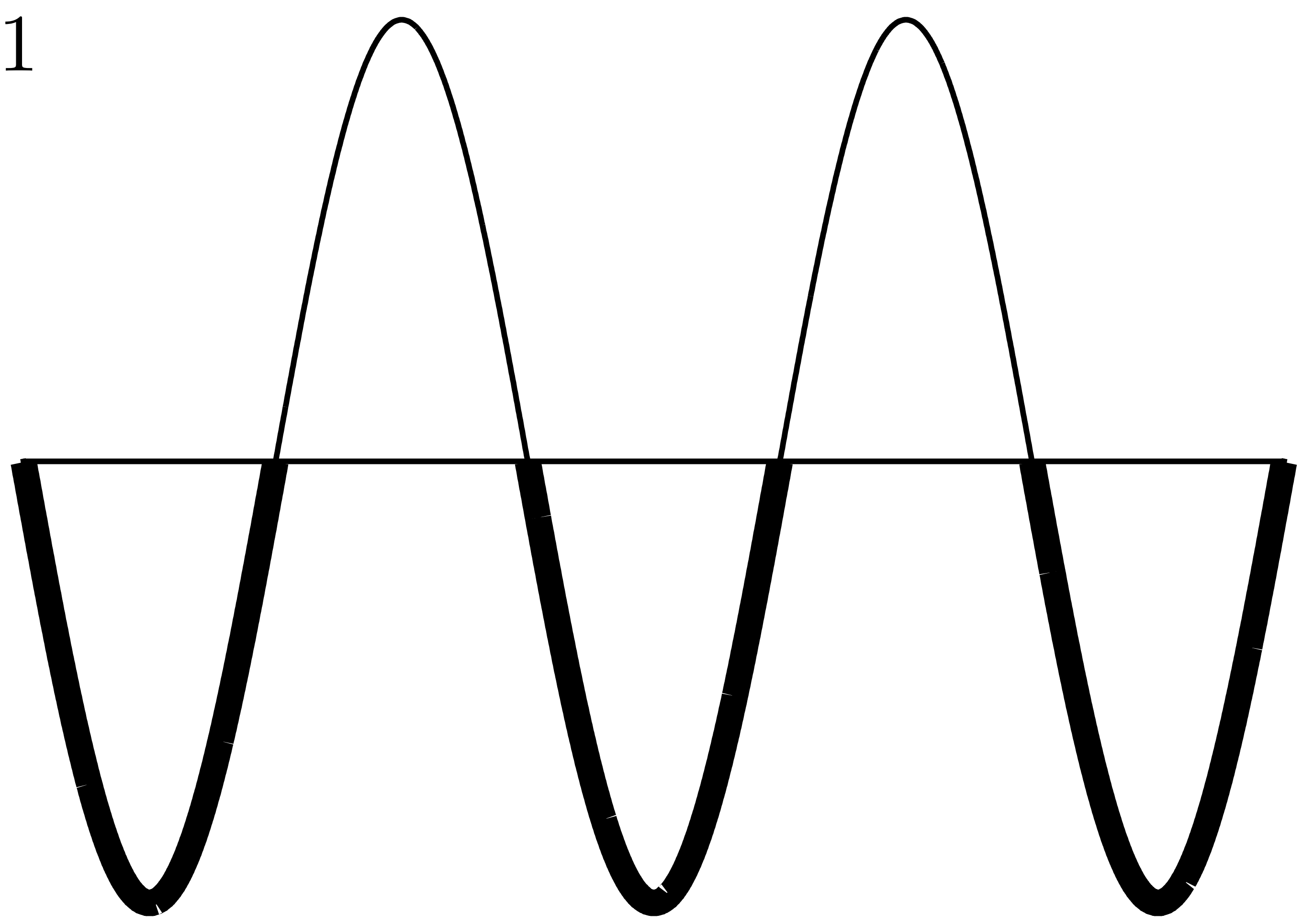

- Renormalized dispersion

$$\overline{\epsilon_k} = \frac{\Omega}{2\pi}\int_0^{2\pi/\Omega} dt \epsilon_{k-A(t)} = \mathcal{J}_0(E/\Omega)\epsilon_k$$

# 1. Origin of the attractive interaction

- Periodic E-field leads to a population inversion

$$\mathcal{J}_0(E/\Omega) = 0.8$$

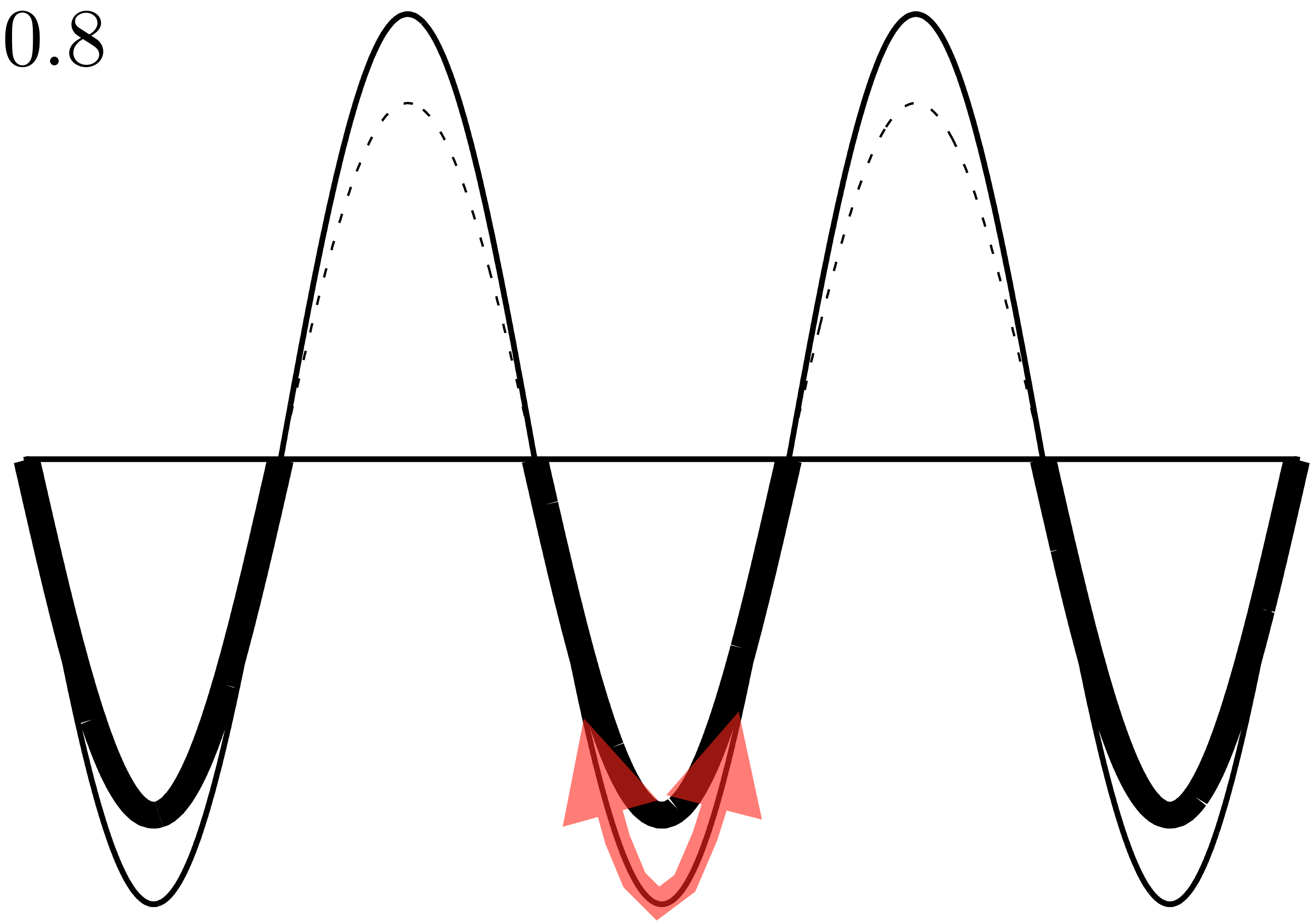

- Renormalized dispersion

$$\overline{\epsilon_k} = \frac{\Omega}{2\pi}\int_0^{2\pi/\Omega} dt \epsilon_{k-A(t)} = \mathcal{J}_0(E/\Omega)\epsilon_k$$

# 1. Origin of the attractive interaction

- Periodic E-field leads to a population inversion

$\mathcal{J}_0(E/\Omega) = 0.3$

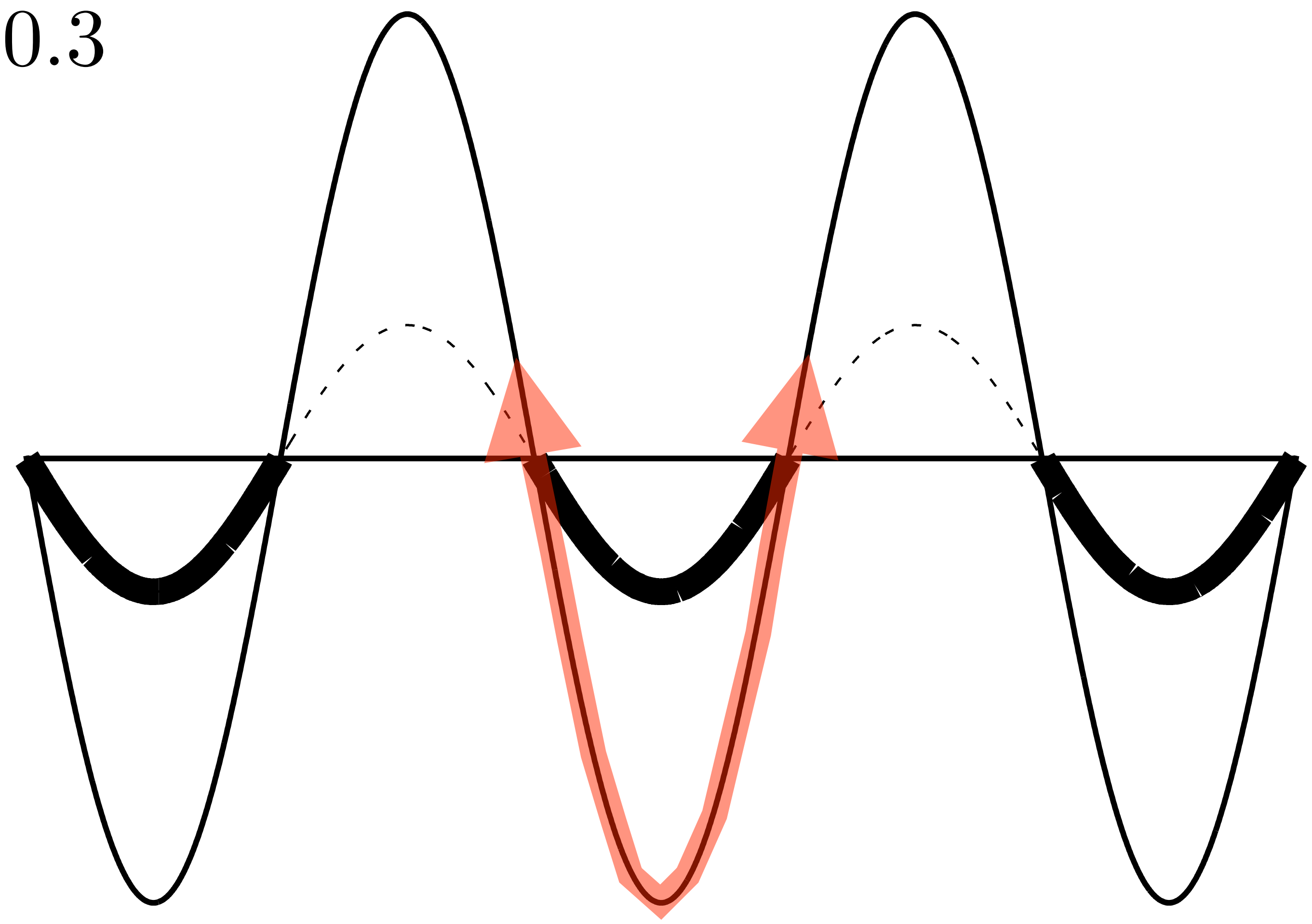

- Renormalized dispersion

$$\overline{\epsilon_k} = \frac{\Omega}{2\pi}\int_0^{2\pi/\Omega} dt \epsilon_{k-A(t)} = \mathcal{J}_0(E/\Omega)\epsilon_k$$

# I. Origin of the attractive interaction

- Periodic E-field leads to a population inversion

$$\mathcal{J}_0(E/\Omega) = -0.2$$

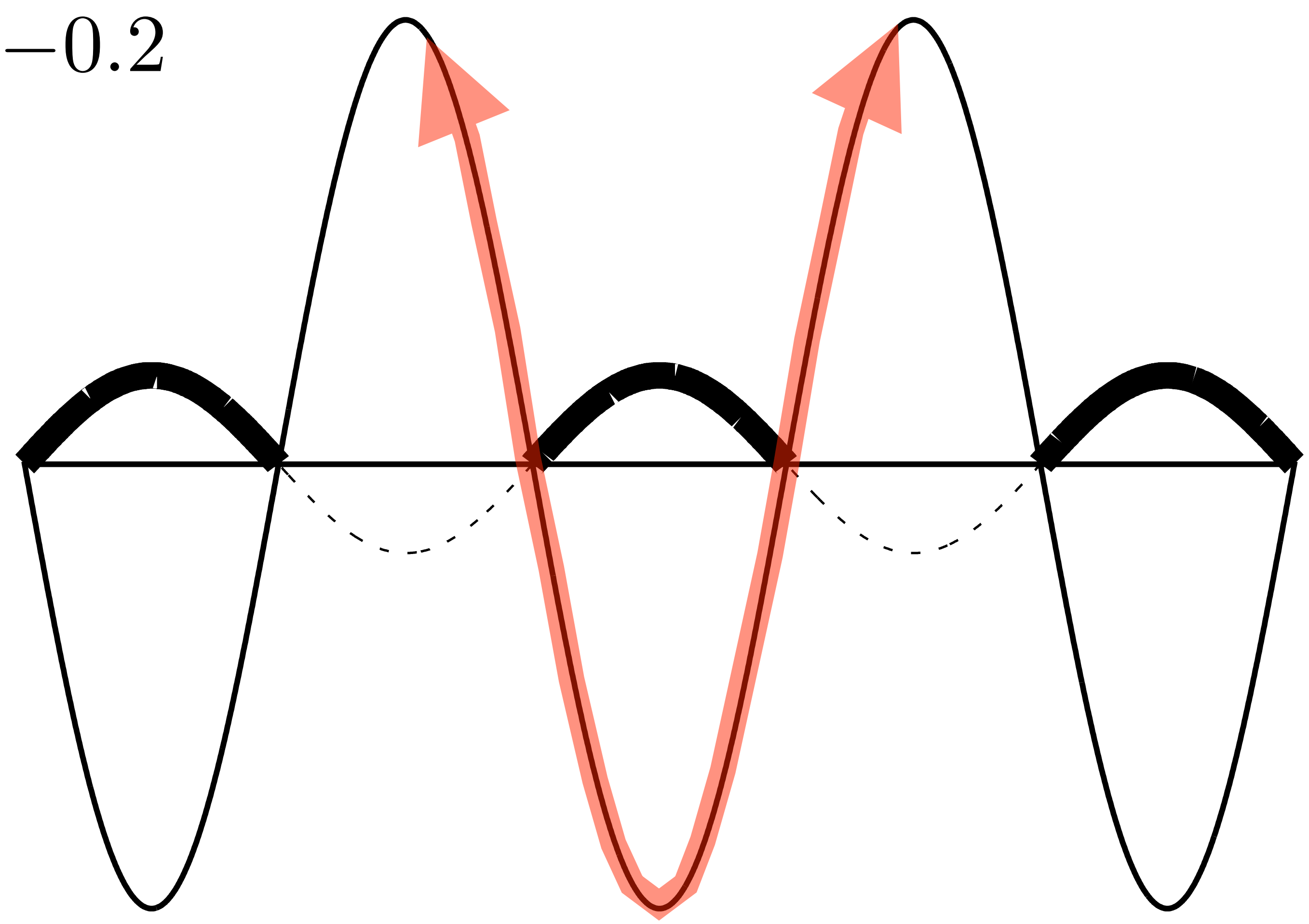

- Renormalized dispersion

$$\overline{\epsilon_k} = \frac{\Omega}{2\pi}\int_0^{2\pi/\Omega} dt\,\epsilon_{k-A(t)} = \mathcal{J}_0(E/\Omega)\epsilon_k$$

# I. Origin of the attractive interaction

- Inverted population = negative temperature

- State with $U > 0, T < 0$ is equivalent to state with $U < 0, T > 0$

$$\tilde{T} < 0, \mathcal{J}_0 < 0 \qquad \rho \propto \exp\left(-\frac{1}{\tilde{T}}\left[\sum_{k\sigma} \mathcal{J}_0 \epsilon_k n_{k\sigma} + U \sum_i n_{i\uparrow} n_{i\downarrow}\right]\right)$$

$$T_{\text{eff}} = \frac{\tilde{T}}{\mathcal{J}_0} > 0 \qquad = \exp\left(-\frac{1}{T_{\text{eff}}}\left[\sum_{k\sigma} \epsilon_k n_{k\sigma} + \frac{U}{\mathcal{J}_0} \sum_i n_{i\uparrow} n_{i\downarrow}\right]\right)$$

- Effective interaction of the $T_{\text{eff}} > 0$ state

$$U_{\text{eff}} = \frac{U}{\mathcal{J}_0(E/\Omega)}$$

# 1. Effect on superconductivity

- AC-field quench from $U = 1$ to $U_{\text{eff}} = -2.5$ (NCA solver)

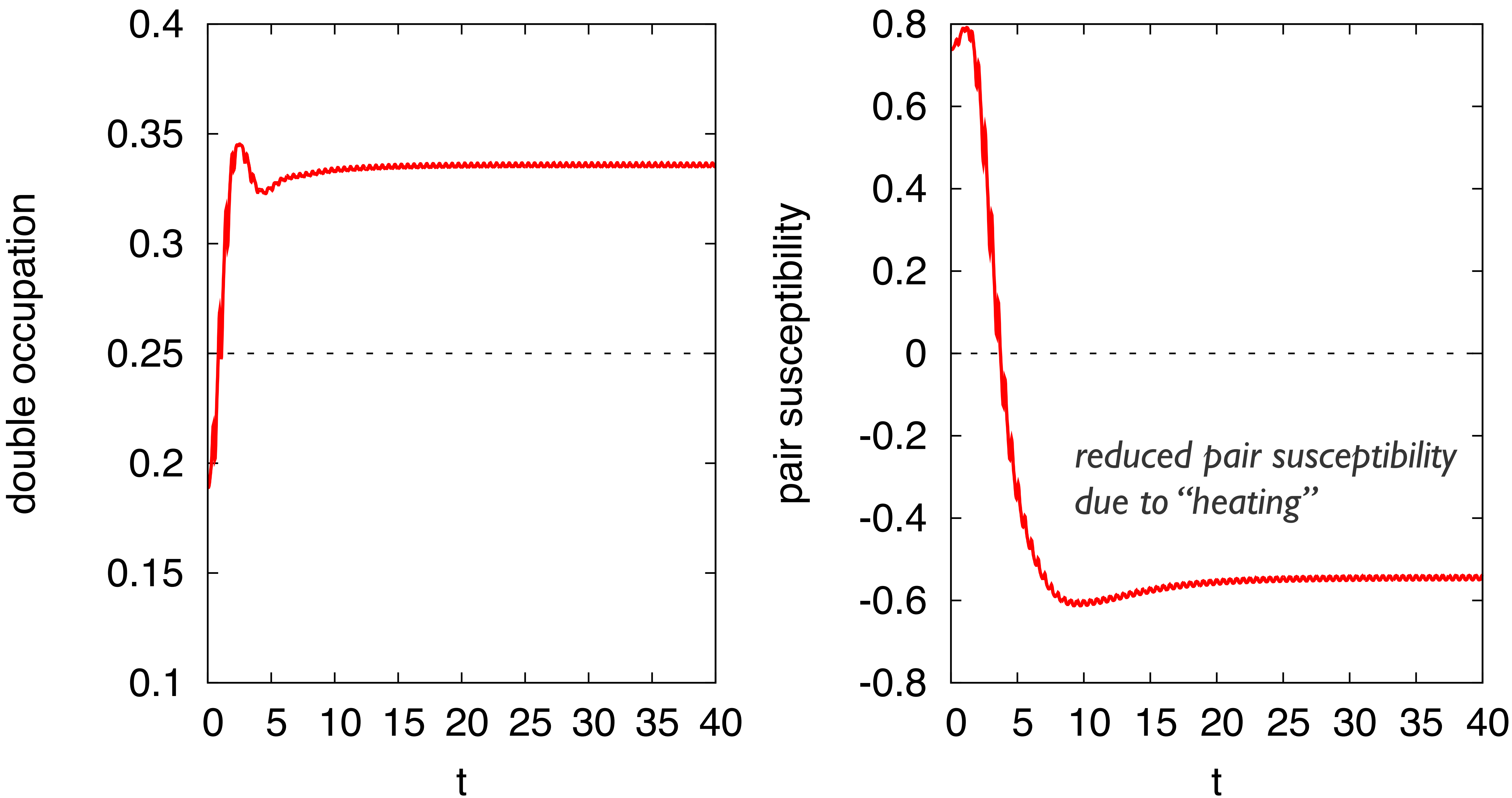

# II. Nonthermal symmetry-broken states

- Equilibrium DMFT phase diagram (half-filling)
- Half-filling: transformation $c_{i\uparrow} \to c_{i\uparrow}^\dagger \quad (i \in A), \quad c_{i\uparrow} \to -c_{i\uparrow}^\dagger \quad (i \in B)$ maps repulsive model onto attractive model

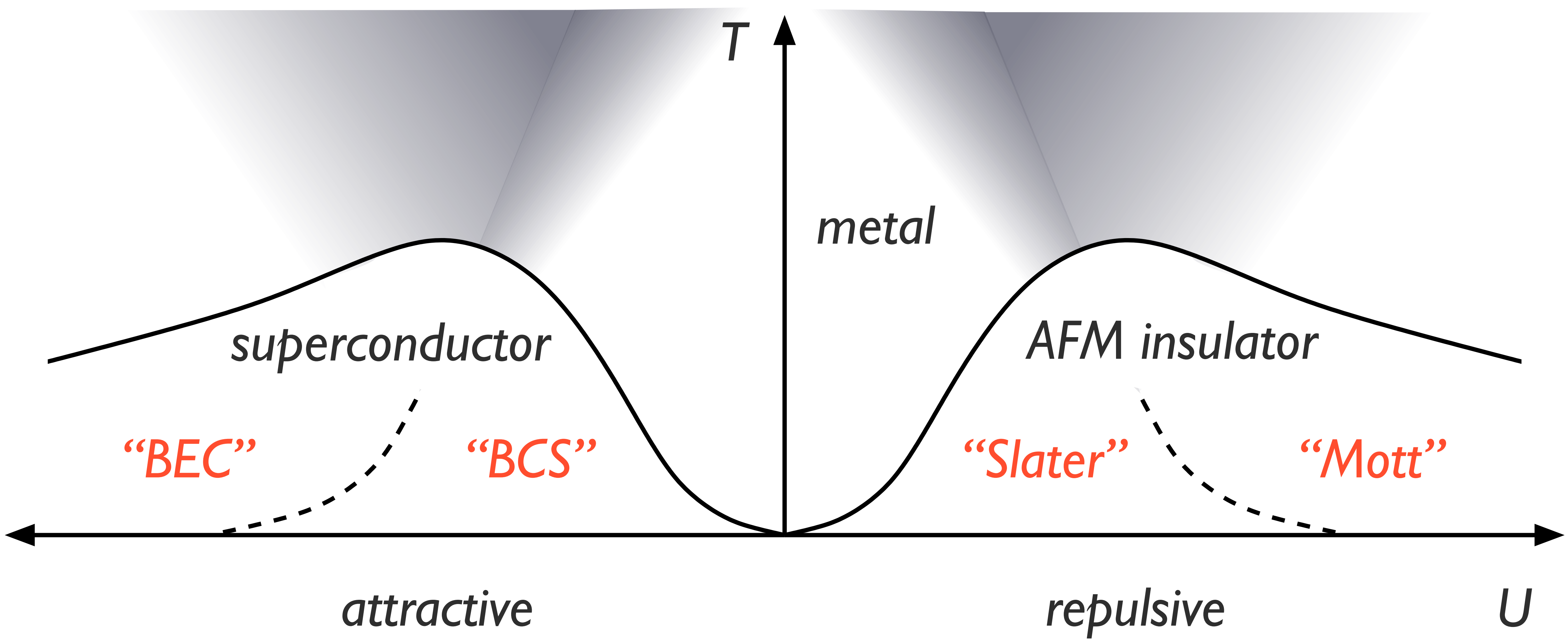

# II. Nonthermal symmetry-broken states

- Weak-coupling regime

  *Tsuji, Eckstein & Werner, PRL 110, 136404 (2013)*

- Slow ramp from (Slater-)Antiferromagnet to Paramagnet

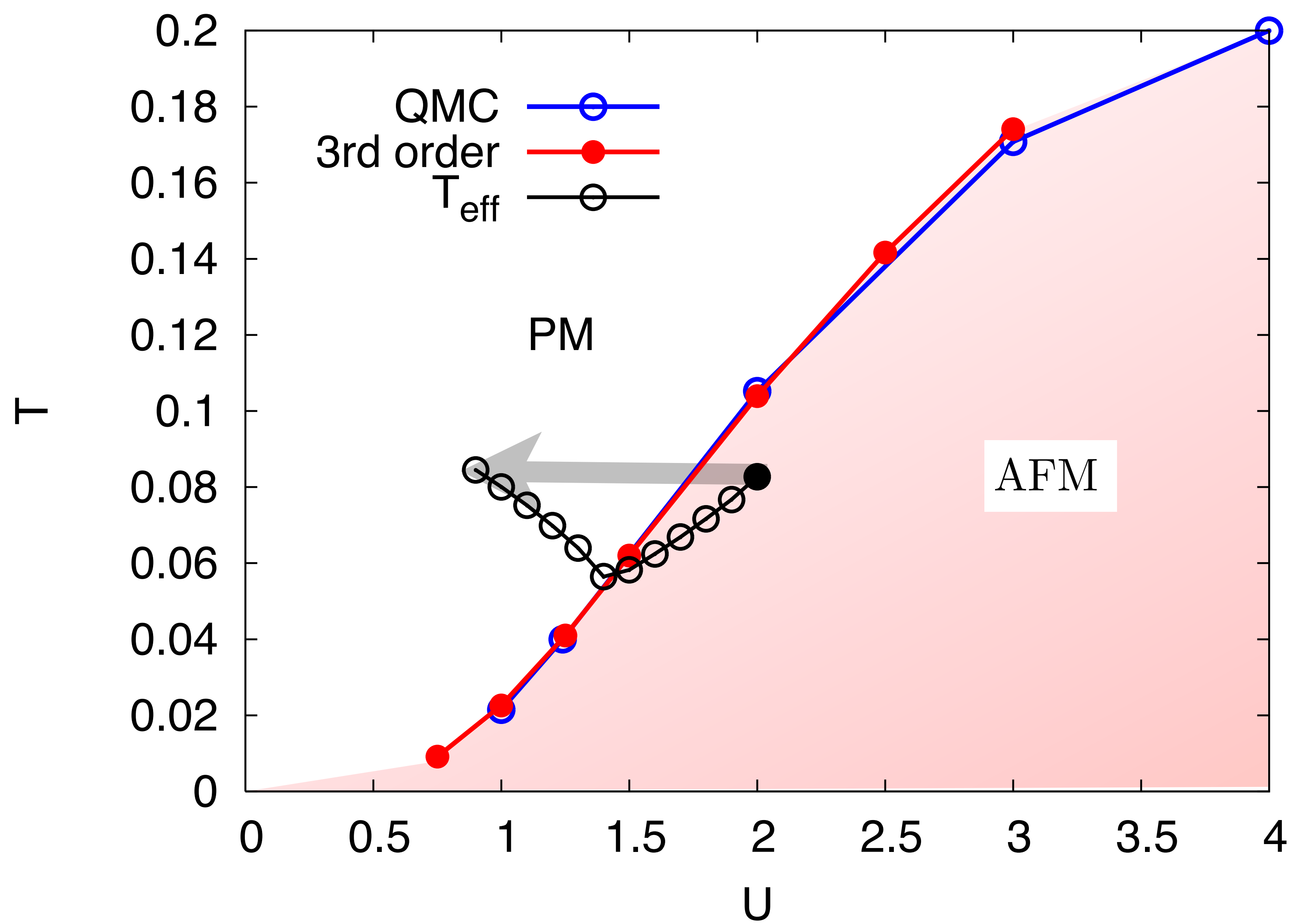

# II. Nonthermal symmetry-broken states

- Weak-coupling regime

  *Tsuji, Eckstein & Werner, PRL 110, 136404 (2013)*

- Time-evolution of the magnetization for different final *U*

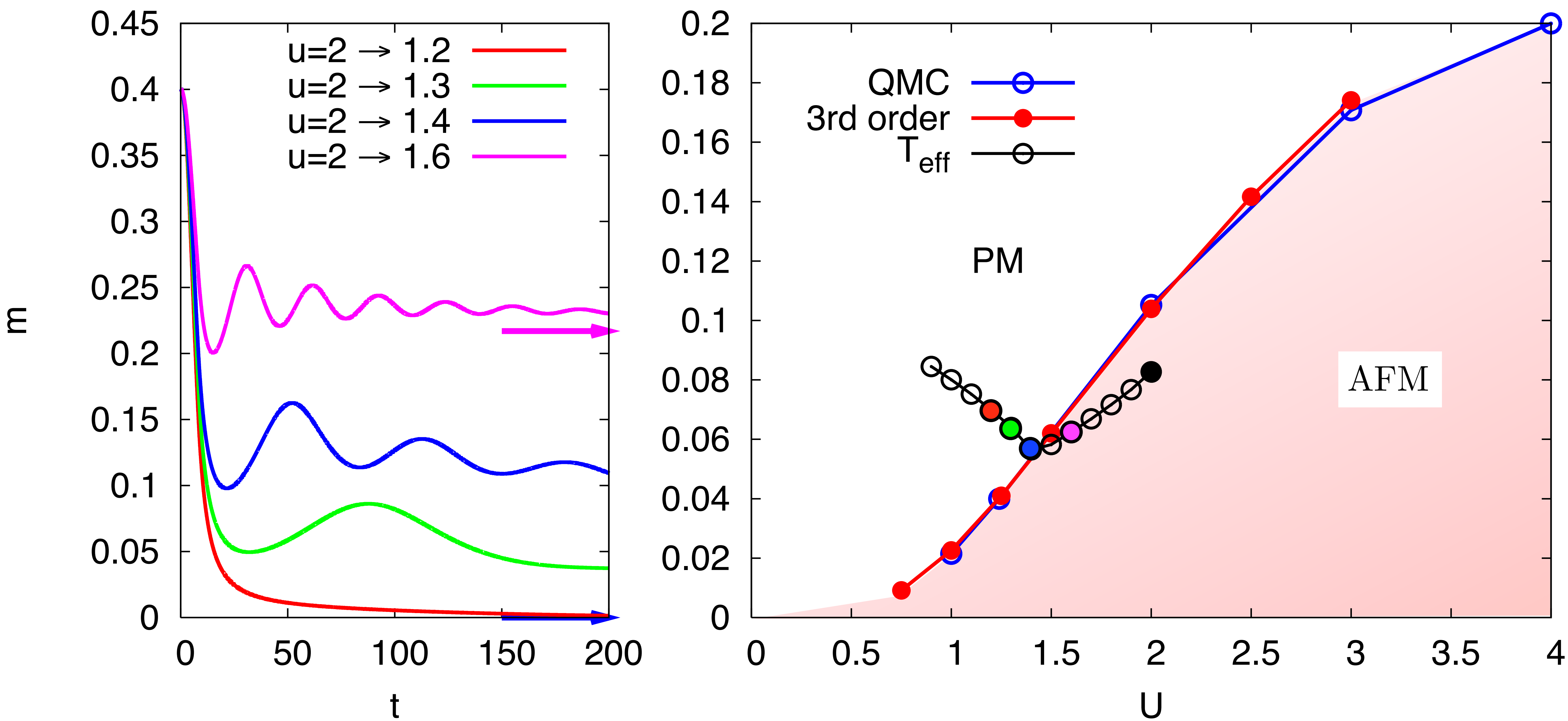

# II. Nonthermal symmetry-broken states

- Weak-coupling regime

  *Tsuji, Eckstein & Werner, PRL 110, 136404 (2013)*

- Time-evolution of the magnetization for different final *U* (Hartree)

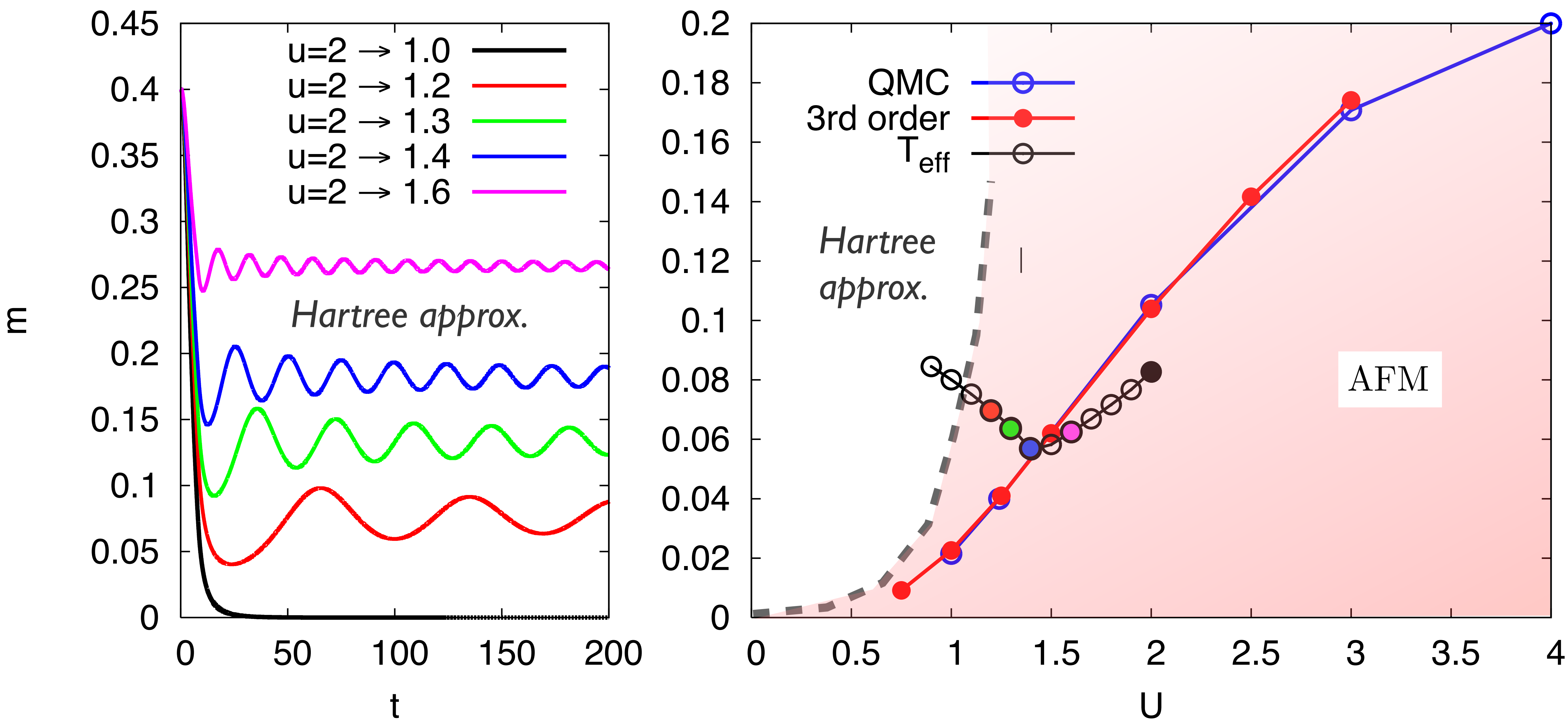

# II. Nonthermal symmetry-broken states

- Weak-coupling regime

  *Tsuji, Eckstein & Werner, PRL 110, 136404 (2013)*

- Time-evolution of the magnetization for different final *U*

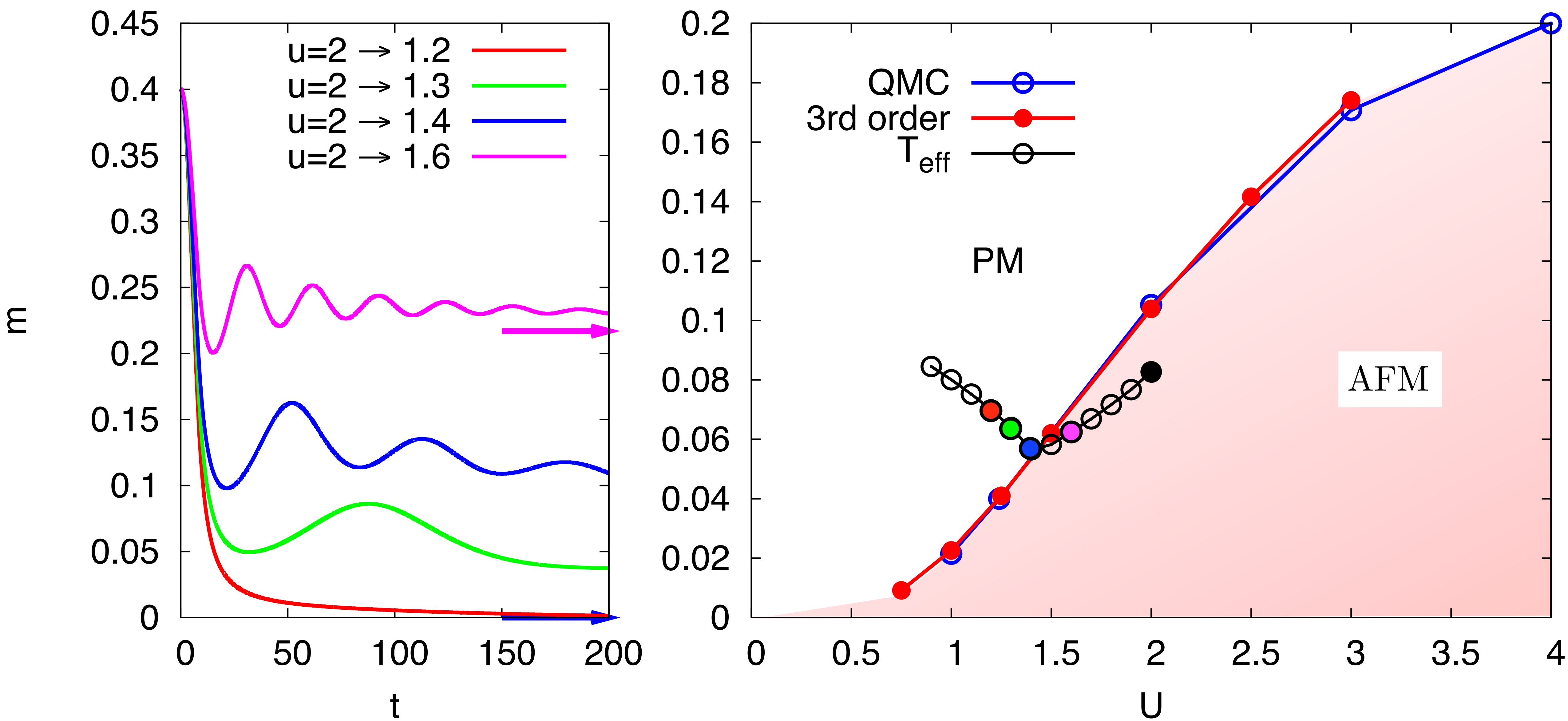

# II. Nonthermal symmetry-broken states

- Weak-coupling regime

  *Tsuji, Eckstein & Werner, PRL 110, 136404 (2013)*

- Evidence for a nonthermal critical point

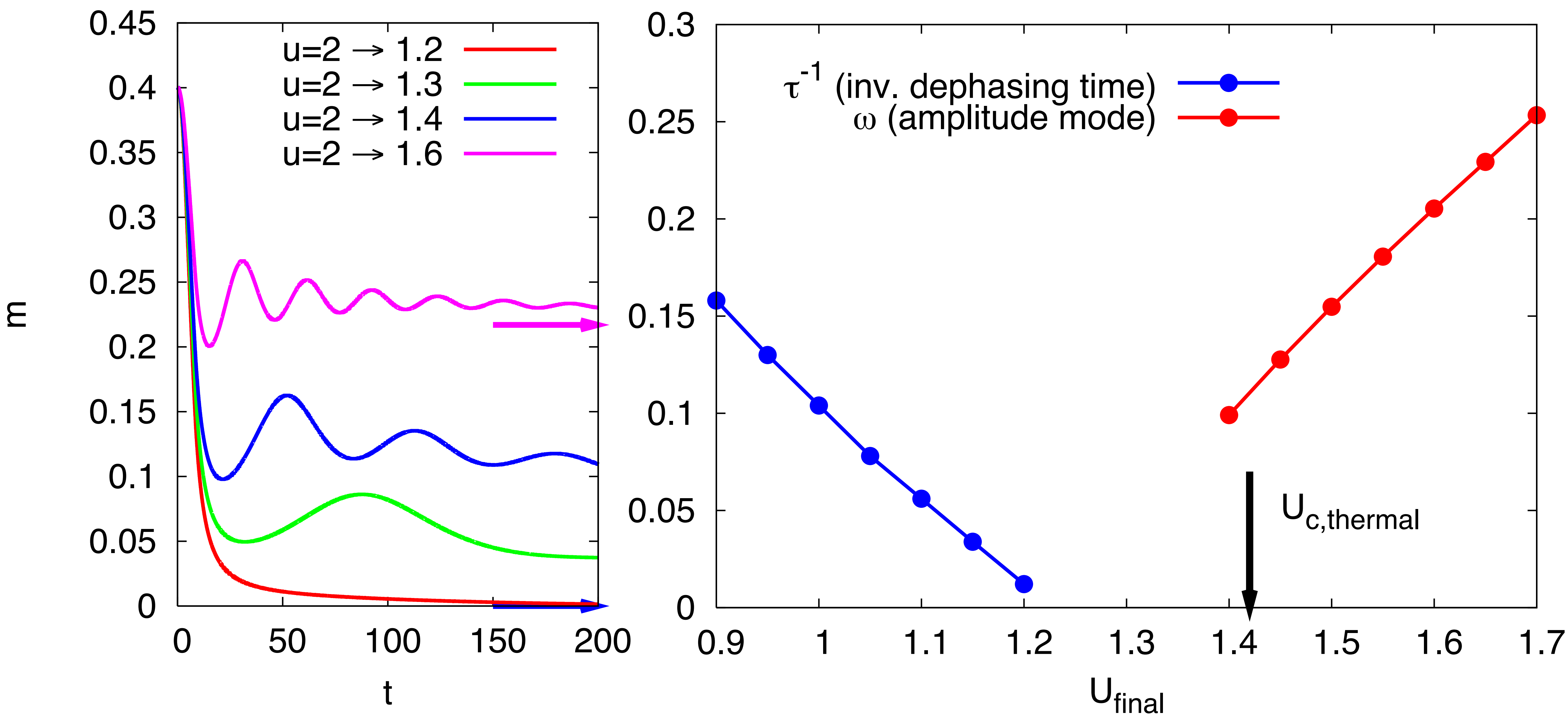

# II. Nonthermal symmetry-broken states

- Weak-coupling regime

  *Tsuji, Eckstein & Werner, PRL 110, 136404 (2013)*

- Evidence for a nonthermal critical point

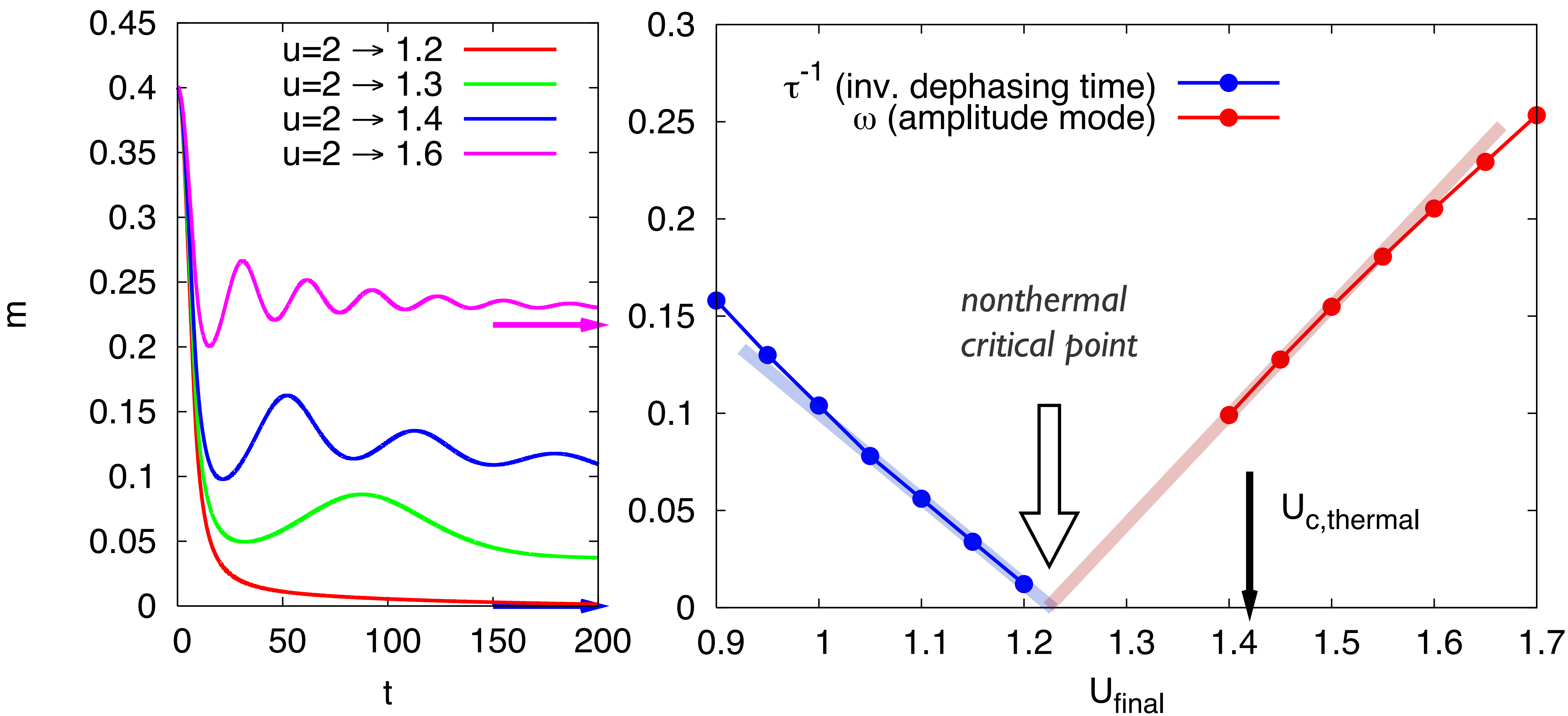

# II. Nonthermal symmetry-broken states

- Weak-coupling regime

  *Tsuji, Eckstein & Werner, PRL 110, 136404 (2013)*

- Evidence for a nonthermal critical point

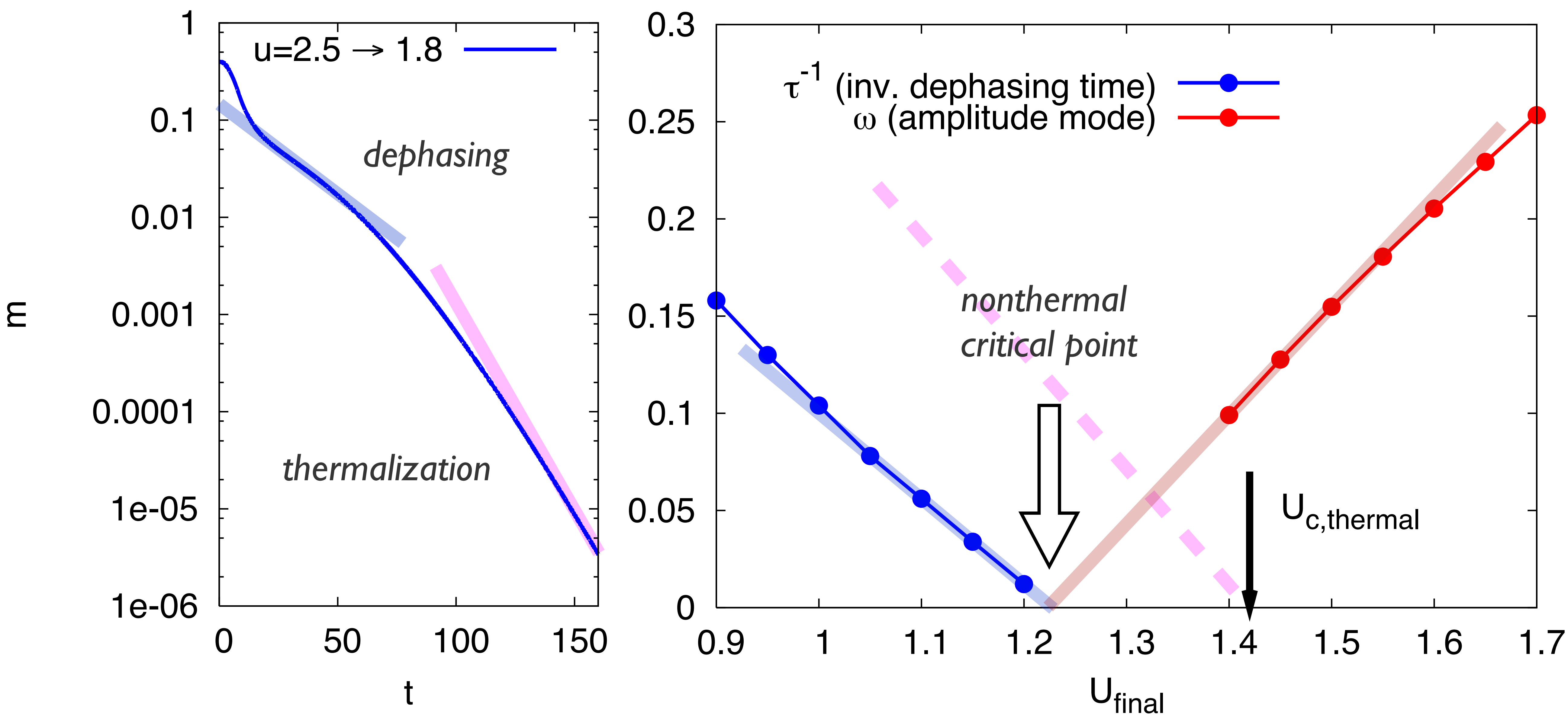

# II. Nonthermal symmetry-broken states

- Weak-coupling regime

  *Tsuji, Eckstein & Werner, PRL 110, 136404 (2013)*

- Evidence for a nonthermal critical point

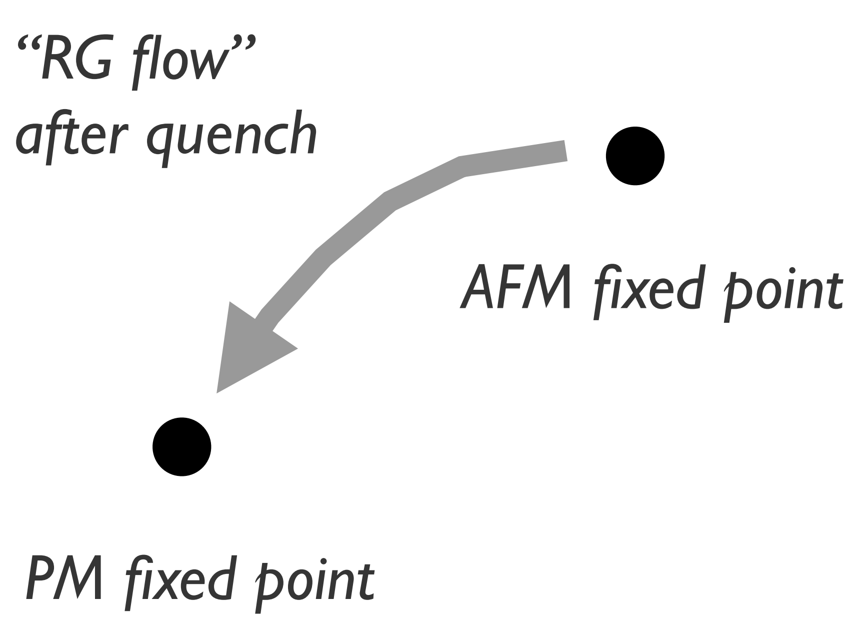


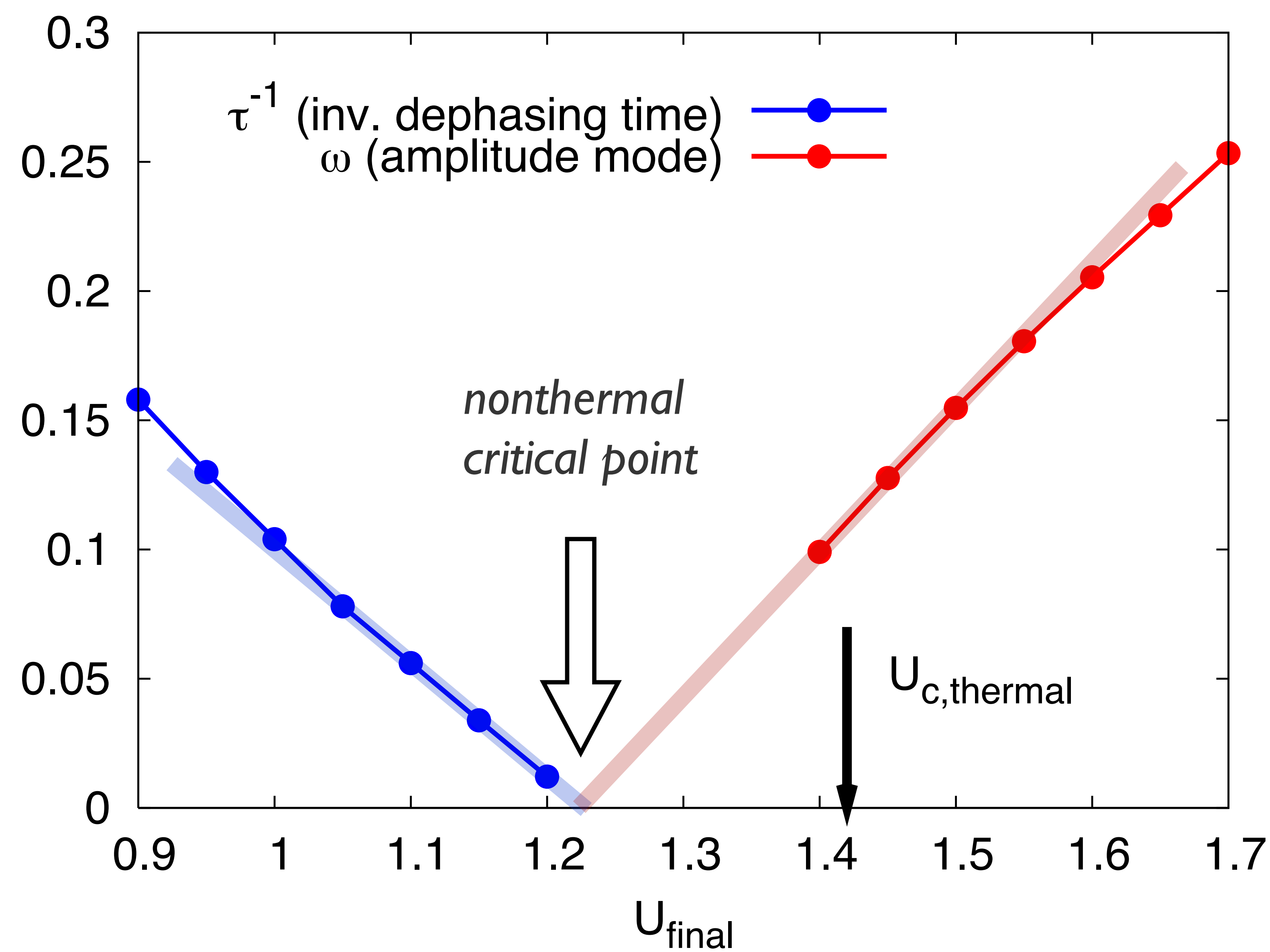

# II. Nonthermal symmetry-broken states

- Weak-coupling regime

  *Tsuji, Eckstein & Werner, PRL 110, 136404 (2013)*

- Evidence for a nonthermal critical point

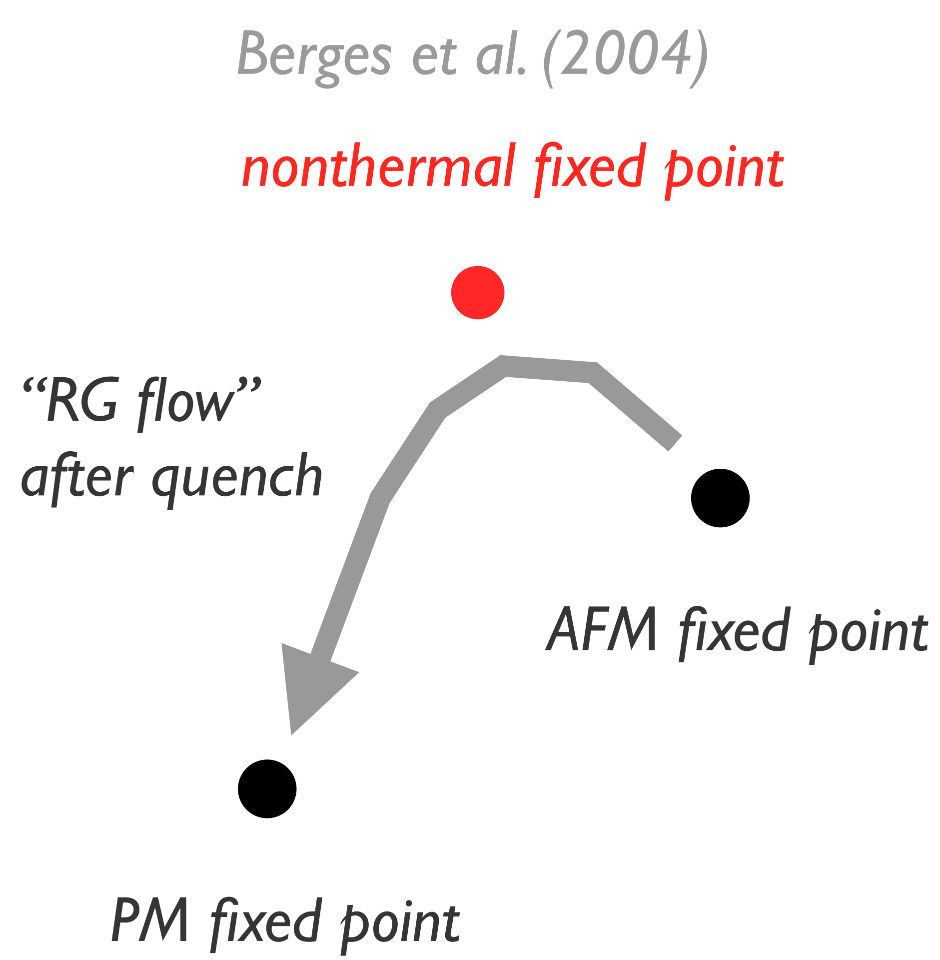


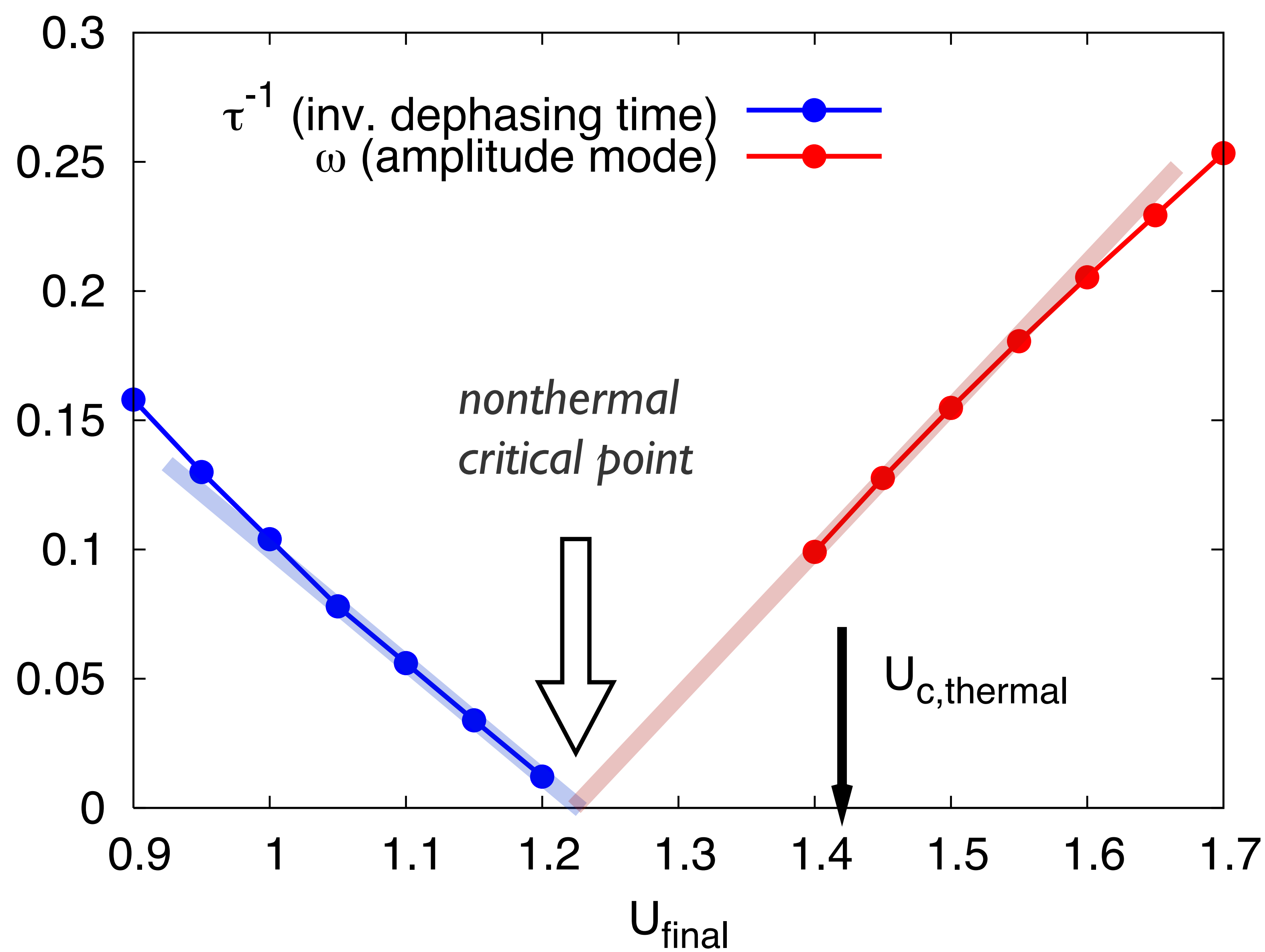

# Summary

- Two examples

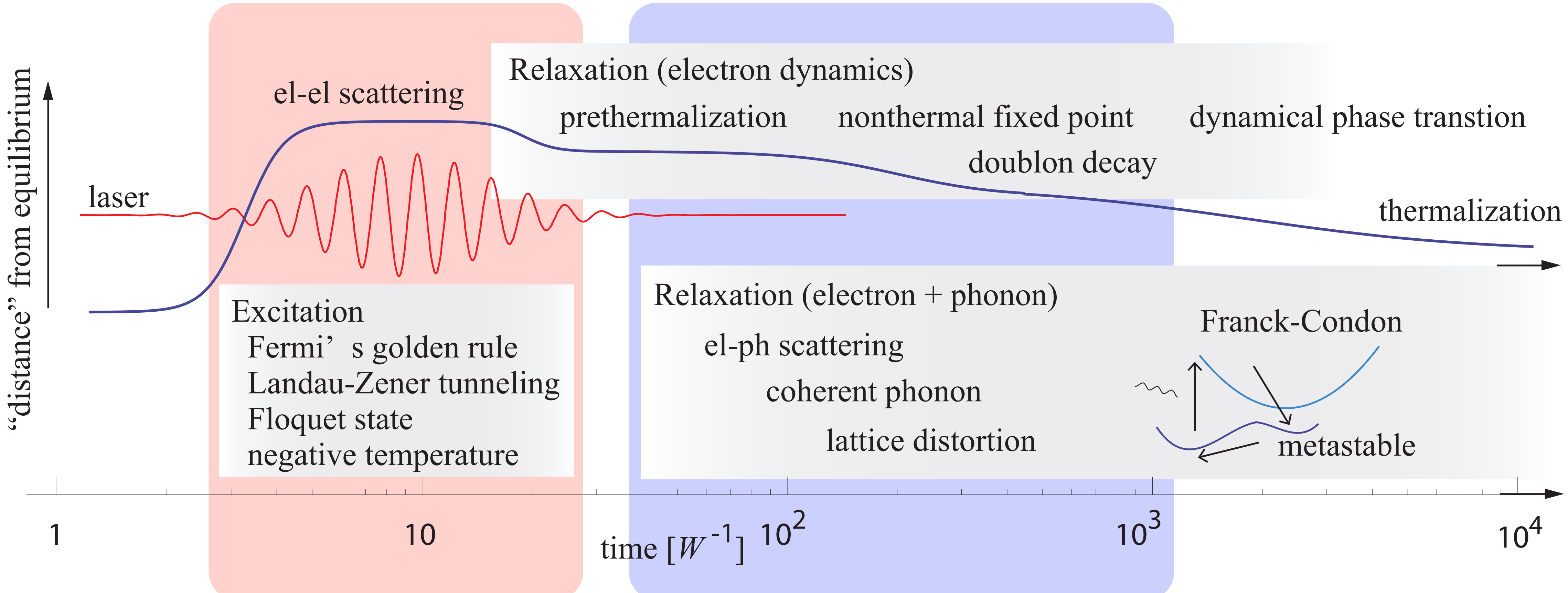


I. Floquet state

Dynamical band flipping and repulsion-to-attraction conversion

II. Dynamical phase transition

Trapped antiferromagnetic order and nonthermal "Hartree" fixed point

# References

- Dynamical mean field theory of strongly correlated fermion systems and the limit of infinite dimensions

  A. Georges *et al.*, Rev. Mod. Phys. 68, 13 (1996)

- Nonequilibrium dynamical mean field theory and its applications

  H. Aoki *et al.*, Rev. Mod Phys. 86, 779 (2014)

- Acknowledments:

  Martin Eckstein (Erlangen), Marcus Kollar (Augsburg), Naoto Tsuji (RIKEN), Takashi Oka (Dresden), Hideo Aoki (Tsukuba), Hugo Strand, Denis Golez (New York), Yuta Murakami (Tokyo)